

Emergence of simple patterns in many-body systems: from macroscopic objects to the atomic nucleus

R.F. Garcia Ruiz^{1,2 a} and A.R. Vernon^{3,4 b}

¹ CERN, CH-1211 Geneva 23, Switzerland

² Massachusetts Institute of Technology, Cambridge, MA 02139, USA

³ KU Leuven, Instituut voor Kern- en Stralingsfysica, B-3001 Leuven, Belgium

⁴ School of Physics and Astronomy, The University of Manchester, Manchester M13 9PL, United Kingdom

Received: date / Revised version: date

Abstract. Strongly correlated many-body systems often display the emergence of simple patterns and regular behaviour of their global properties. Phenomena such as clusterization, collective motion and appearance of shell structures are commonly observed across different size, time, and energy scales in our universe. Although at the microscopic level their individual parts are described by complex interactions, the collective behaviour of these systems can exhibit strikingly regular patterns. This contribution provides an overview of the experimental signatures that are commonly used to identify the emergence of shell structures and collective phenomena in distinct physical systems. Examples in macroscopic systems are presented alongside features observed in atomic nuclei. The discussion is focused on the experimental trends observed for exotic nuclei in the vicinity of nuclear closed-shells, and the new challenges that recent experiments have posed in our understanding of emergent phenomena in nuclei.

PACS. XX.XX.XX No PACS code given

1 Introduction

Our understanding of the universe is intimately related to our description of many-body systems. The knowledge of the fundamental particles and forces of nature is as important as our ability to understand how these building blocks are organized to form complex systems. Remarkably, the emergence of simple and regular patterns are common features observed in strongly correlated many-body systems [1–9]. At the microscopic level, the individual parts of different physical systems can be described by fundamentally different interactions, however, their collective behaviour can exhibit similar patterns. These seemingly simple regularities of certain properties of a physical system tends to suggest the existence of underlying symmetries and allows simple models to provide a good description of the observed data [9–13]. However, the link between these models and their microscopic interactions is an open question in many fields of physics.

The over the past decade experimental and theoretical developments have allowed an unprecedented connection between reductionist and emergent views of nature. Advances in many-body methods and the rapid development of computing power have provided new paths towards the ab-initio description of macroscopic phenomena. Theoret-

ical developments are motivated by the ambition of a first principles description of emergent phenomena, yet this reductionist approach is deeply motivated by empirical observations [14,15]. A deeper understanding of the microscopic origin of emergent physical phenomena is achieved through systematic experimental studies confronted with the theoretical descriptions. This article presents a short overview of experimental signatures that are commonly used to characterize the emergence of phenomena in different physical systems. Various examples of objects from the human size scale down to the femtometer scale are presented. The discussion is centered on the observables that are used to indicate the emergence of phenomena such as shell structures and “magic” numbers - integer number of constituents with notably different properties. Albeit not exhaustive, an effort is made to include citations that could be useful to direct interested readers to the relevant literature.

The manuscript is divided in two main parts: The first part provides a brief description of selected examples that illustrate the emergence of regular patterns in macroscopic systems and some of their commonalities and differences with similar patterns observed in the atomic nucleus. The second part is focused on the experimental signatures used to discuss the emergence of collective phenomena and shell structures in nuclei. Commonly discussed properties such as binding energies, nuclear charge radii, excitation ener-

^a E-mail: rgarcia@mit.edu

^b E-mail: adam.vernon@kuleuven.be

gies and transition probabilities are presented. The discussion is expanded using recent experimental results obtained for the ground-state properties of nuclei in the neighborhood of nuclear shell closures. Finally, an emphasis is made on the trends and open questions that the new observations pose for our current understanding of nuclear structure in different regions of the nuclear chart.

2 Emergence of simple patterns in many-body systems

Throughout nature, driving forces give rise to optimization problems for the arrangement of constituents in many-body systems at almost every size scale, resulting in an abundance of emergent phenomena [1–5, 7, 21–34]. On biological scales, despite separation from the smallest constituents of matter by approximately 15 orders of magnitude, simple collective phenomena and pattern formation are still immediately apparent [1, 35–38]. Such as in the phyllotaxis of plants [33, 39, 40], where simple growth patterns appear in the arrangement of leaves or flowers around a plant stem. One particularly striking example is observed in the growth of seeds in a sunflower head [21, 22], in which the number of spirals of seeds follows the Fibonacci sequence. A large variety of patterns emerge in smaller systems as a consequence of the optimal arrangement of their constituents [35, 36, 41], from the clustering in framboidal pyrite [42, 43] to the crowding of molecules in cells [32, 44, 45], or that of DNA strands in cell nuclei [31, 46]. Complex many-body systems often form clusters to minimise their energy by interactions between their neighbours and their mean field. This situation can give rise to “magic” numbers, as with those in the atomic nucleus, where certain integer numbers of constituents of a given system results in greater stability of its collective whole.

The simplest signature for these magic numbers is the greater natural abundance of systems with certain number of constituents [7, 23–25, 25–27, 54]. This is comparable with the abundance distribution of isotopes in the universe [67, 68] following nucleosynthesis [69]. A summary of different systems in nature which exhibit greater stability for certain number of constituents is shown in Table 1, where typical experimental signatures and system sizes are highlighted. Examples of the size scale and driving forces in different many-body systems are illustrated in Figure 1, where the driving forces refer to those essential for the appearance of the magic numbers in these many-body systems. While gravity, for instance, will have only a minor influence. The commonality between all of these systems which exhibit magic numbers appears to be: i. a uniformity in the type of constituents; ii. a subtle balance between attractive and repulsive effective forces, which are either self-generated or from an external mean field. For constituents with their packing constrained by symmetric polyhedral shapes, the magic numbers that appear can be determined for a system with constituents of any size using purely symmetries of geometry, and they appear in nature

with these numbers when this is the case [1, 25, 29, 70–72]. Those constituents between magic numbers, can also be said to belong to a ‘shell’, as with the electronic shells of atoms [56] or for nucleons in atomic nuclei [73, 74]. In some cases this is reflected by the spatial arrangement of the constituents. For example in ‘dusty’ plasmas [75, 76], where charged dust particles (on the micrometer scale) can self assemble into a plasma crystal arrangement with a radial spherical shell distribution of particles [3, 77], with the total system on the scale of millimeters. Such mesoscopic systems are often called ‘artificial atoms’ due to their close resemblance with atomic systems. The magic numbers listed in Table 1 for dusty plasmas, occur for particular experimental conditions. These experiments have several highly tunable parameters, which can result in different sequences of magic numbers [77–79], highlighting the ability of a magic number sequence to reflect the underlying interactions of a given system.

Self arrangement and the appearance of magic numbers has also been observed in 2-dimensional mesoscopic experiments using micrometer-sized superconducting disks [4, 80]. At the scale of hundreds of micrometers, polystyrene spheres (colloidal particles) with diameters of around 200 nm have been observed to self-assemble into colloidal clusters [81, 82]. While the interaction has a complicated description including surface chemistry [83], capillary forces [84], entropy maximization [82] and the presence of depletants [85]. These clusters were found to form certain magic number configurations during a drying process [5], these configurations were found to have higher thermodynamic stability. These particularly stable configurations of clusters are found to form upon confinement described mainly by a short-range repulsive potential, and weak attractive interactions between colloidal particles [5]. Due to the absence of a long-range repulsive force (such as the Coulomb force which limits the size of atomic nuclei) between the colloidal particles, these colloidal systems can range from a few particles [84] to billions of particles (colloidal crystals) [86, 87].

Perhaps the systems with the most in common with the atomic nucleus are atomic clusters [9, 19, 88], an area of physics which has historically benefited from analogies with nuclear models [19, 89, 90]. Clusters of atoms were observed to have magic numbers of enhanced stability reflected in their produced mass abundance spectra [25–27, 91] (see Table 1). The electronic structure of the constituent atom ultimately dictates the properties of the atomic clusters, however phenomenological models have been developed to provide a good description of the observed magic numbers, similar to the shell model of the atomic nucleus [8, 92]. A ‘wine-bottle’ shaped potential used to describe these atomic clusters was adapted from the Woods-Saxon potential of nuclear physics [91]. This potential predicted ‘super shells’ to appear as the number of atoms in the clusters approaches $N = 1000$ [90], due to higher-order stabilizing effects, analogous to the predicted islands of stability of heavy nuclei [93, 94]. The predicted super-shell magic numbers were soon observed in sodium clusters [28]. Deformation also has an analo-

Table 1. Experimental signatures of the emergence of shell structures and “magic” numbers in different many-body systems. The size scales and the common observables that are used to characterize the properties of each systems are indicated. Here the ellipses (“...”) are used to denote that additional magic numbers have been omitted for space.

Constituent	Size	System	Size	r_c	Observable(s)	Magic numbers	Refs.
Spheres	Any	Spherical packing	Any		Density	6, 12, 21, 25, 38 ...	[1]
Sunflower seeds	~ 1 cm	Sunflower head	5-50 cm	~ 4 mm	Number of spirals	3, 5, 8, 13, 21, 34, ...	[2, 21, 22]
Dust particles	μm	3D plasma crystal	mm	400 -760 μm	Radial distribution	2, 21, 60, 107 ..	[3]
Superconducting disks	μm	Vortex shells	5 μm	$\sim 2 \mu\text{m}$	Radial distribution	5, 16, 32	[4]
Polystyrene spheres	244 nm	Colloidal cluster	2-8 μm	136 -156 nm	Evaporation rate	135, 297, 851, 801, 1283, 2583 ...	[5]
GaAs layers	10 nm	Quantum dot	0.5 μm	7 -10 nm	Electron addition energy	2, 6, 12, 20 ...	[47]
Virus protein	~ 5 nm	Virus capsids	20 -400 nm	2 -10 nm	Abundance	15, 17, 18, 42	[48-52]
C atoms	170 pm	Fullerenes	0.5 -2 nm	70 -110 nm	Mass abundance	60, 70, 72, 76, 78, 84 ..	[7, 23, 24, 53]
H ₂ O	275 pm	Electron-bound water clusters	~ 3 -20 Å	170 -190 pm	Mass abundance	2, 6, 7, 11	[54]
Xe atoms	216 pm	Atom clusters	~ 2 -10 Å	158 -264 pm	Mass abundance	13, 16, 19, 25, 55, 71, 87, 147 ...	[25, 26]
Na atoms	227 pm	Atom clusters	~ 2 -10 Å		Mass abundance Ionization energy Melting temperature	2, 8, 20, 40, 58, 92 ... 55, 116, 147, 178 ...	[27, 28, 55] [29]
Electrons	fm	Atoms	31 -348 pm	20 -70 pm	Binding energies	2, 10, 18, 36, 54	[56]
Nucleons	fm	Nuclei	1-10 fm	~ 1.2 fm	Binding energies, $t_{1/2}$, $\langle r^2 \rangle$, B(E2), E_{2+} , Q_S , μ , Solar abundances, Neutron capture σ s	2, 8, 20, 28, 50, 126 ..	[57-61] [62] [63] [64] [6, 65] [61, 66]

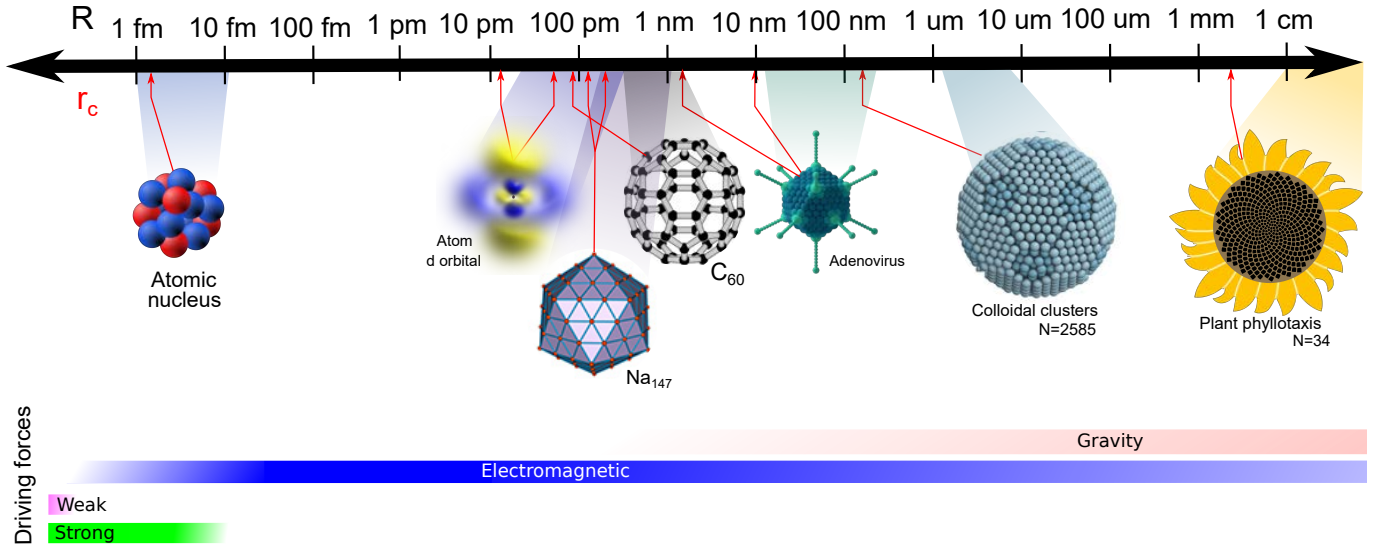


Fig. 1. Size scale, R , characteristic length, r_c and main driving forces are compared for different many-body systems including sunflower seed phyllotaxis [16], colloidal clusters [5], virus capsid structures [17], fullerenes [18], metal clusters [19], atoms [20] and atomic nuclei (Color online).

gous role in these clusters as in atomic nuclei, where the most stable clusters have spherical deformation and those between shell closures have oblate or prolate deformation [8,9]. The Nilsson model of the atomic nucleus [95] has been adapted to describe axially deformed clusters, known as the Clemenger-Nilsson model [96]. Giant dipole resonances of atomic nuclei [97] also have a counterpart in these cluster systems, in the form of plasma resonance frequencies [98,99]. Taking the example of the sodium clusters, many of the observables corroborate the same set of magic numbers [27, 55, 100–102] which are of electronic origin. A modified set of magic numbers was found in the melting temperatures of the clusters [103] however. This required an additional interpretation considering the geometric shells of the positions of the atomic nuclei alongside the electronic shells, due to the importance of the positions of the atomic nuclei in the melting process [29].

In the fermionic systems, the Wigner-Seitz radius, r_c , is commonly introduced to characterize the length scale of a system (see Ref. [104] for a detailed discussion of fermionic many-body systems). It is defined as the radius of a sphere whose volume is equal to the mean volume per constituent, given by $r_c = R/n^{1/3}$ for 3-dimensional systems with n constituents, and $r_c = R/n^{1/2}$ for 2-dimensional systems. The r_c values for some of the systems discussed here are shown in Table 1. This value also gives an estimate for the density of the systems, which becomes independent of the system size when saturated. This characteristic is particularly important in the understanding of the saturation of nuclear matter, as the r_c value remains nearly constant in finite nuclei, and it remains with a similar magnitude for systems as large as neutron stars [104]. Similarly, other many-body systems with rigid constituents exhibit comparatively small variations in their r_c value with the increase of the system size (see Figure 1).

Fermionic systems such as atomic nuclei, atoms, atomic clusters and quantum dots can be constrained by similar symmetries [105]. The Pauli exclusion principle, common to all of these systems, imposes the first magic number, 2. However the sequences of magic numbers strongly depend on the forces and symmetries that describe their constituents. In the atomic nucleus, the attractive mean-field is self-generated by the constituent nucleons, rather than a common external potential as for electrons in atoms. The ‘spin-orbit’ force between nucleons [73], produces a large attractive force which increases the binding for nucleons in orbital shells with their spins aligned with their orbital angular momentum. Whereas the spin-orbit force between electrons is significantly weaker and repulsive for aligned spin and orbital angular momentum [106].

In the influential paper “More is different” [10], P. W. Anderson argued that as the number of constituents of a system increases, a “phase transition” occurs, where the symmetries of the underlying laws of the system are broken and new symmetries can appear, requiring research into these fundamentally new and different laws of the system on the new hierarchy, as was the case with superconductivity [107]. With this outlook it was said that the “constructionist” approach might be lost, that is the ability to predict the emergent phenomena of a system from fundamental laws of physics. It is accepted that emergent properties in complex systems with large number of constituents can require many-body calculations which are presently computationally infeasible, and thus is impossible to establish a direct connection to the fundamental forces of nature [105, 108]. However, for mesoscopic systems such as atoms and nucleus, the reductionist viewpoint that the system is still in fact reducible to these laws, is becoming feasible thanks to the developments in powerful many-body methods and computational power. The in-

interactions among electrons are well understood in terms of their underlying theory of quantum electrodynamics, and atomic properties can now be calculated with high accuracy for different many-electron systems [109–113]. The non-perturbative nature of the nuclear force makes the atomic nuclei exceedingly more complex, and their description from first principles is an ongoing challenge for nuclear theory [114–119].

3 Global trends and simple patterns in nuclei

The atomic nucleus provides a rich laboratory in the studies of strongly correlated many-body systems. Due to the high nuclear density and the short- and long-range properties of the nuclear force, nuclei are highly sensitive to two- and higher-order many-body forces. The non-perturbative character of the strong force requires highly demanding theoretical treatments. In contrast to other physical systems, three-body forces are essential to describe the properties of nuclei [120]. By varying the numbers of protons and neutrons in the nucleus, inter-nucleon correlations can drive very different collective phenomena [121–124]. Intriguingly, a set of regular patterns appear across the whole nuclear chart [125–130]. These seemingly simple patterns have motivated numerous phenomenological models since the early days of nuclear physics. Simple model principles such as independent-particle motion [131, 132] and the semi-classical collective motion of nuclei [133] have been very successful in providing a global description of the observed nuclear phenomena. Below we present a short overview of the experimental signatures of nuclear shell structures and collective phenomena that are commonly discussed in literature. While similar signatures and correlations are found in several nuclear observables, different patterns can emerge in systems with extreme proton-to-neutron ratios. This discussion is expanded upon using the evolution of nuclear properties in the neighborhood of the neutron-rich ^{52}Ca ($Z = 20$, $N = 32$), ^{78}Ni ($Z = 28$, $N = 50$), and ^{132}Sn ($Z = 50$, $N = 82$) isotopes as examples, where new theoretical and experimental results have become available in the last few years.

3.1 Experimental signatures of shell structures

The signatures of nuclear shell structures are manifested in different observables [123, 127, 134–137]. The numbers of nucleons that completely fills nuclear closed-shells are the so-called “magic” numbers. Nuclei with a magic number of nucleons are commonly observed to have the following experimental signatures: i. a relatively small mean-squared charge radius, $\langle r^2 \rangle$. As seen in Figure 2 at nucleon number $N = 20, 28, 50, 82$ and 126 , there is a pronounced change of the charge radius as nucleons are added beyond a shell closure (“kink”), with a smooth increase towards shell closures, and a larger increase through the filling of the new open shell [128]. ii. a relatively large two-nucleon separation energy, S_{2n} ; iii. a small quadrupole moment value, Q_s ; iv. a high excitation energy of the first 2^+ state, E_{2^+} ;

and v. a small transition probability to the first 2^+ excited state, $B(E2)$. A compilation of these experimental properties as a function of the neutron and proton numbers are shown in Figure 2 and Figure 3, respectively. The data corresponding to different isotones are shown in Figure 2, using bars of different colors to indicate the magnitudes of the observables for each isotone, the same is shown in 3 as a function of atomic number.

The changes of the mean square charge radii when two neutrons are added, $\Delta\langle r^2 \rangle(2n)$, are presented in Figure 2. The analogous differences when two protons are added, $\Delta\langle r^2 \rangle(2p)$, are shown in Figure 3, however the data in this case is relatively sparse as the charge radii of many elements have not yet been measured. At magic number of nucleons these differences exhibit a minimum value, with local maxima occurring after crossing the closed shell. As the magnitude of Q_s , $B(E2)$, and E_{2^+} scales with the atomic number and the nuclear size, these parameters were normalized in order to compare light and heavy nuclei on the same scale. The experimental values of Q_s and $B(E2)$ were scaled to the dimensionless values Q_s/ZR^2 and $B(E2)/Z^2R^2$, with Z the proton number and $R = 1.18A^{1/3}$ the droplet-model radius. Normalized observables present minimum values around the nucleon numbers 28, 50, 82 and 126, with a clear correlation seen in the trends of all observables. For some isotopes, additional local minima appear around nuclear numbers 2, 8, 16, 20, and 40. Figure 2 iv), for example, shows bars of different color at $N = 20$, indicating that nuclei with the same number of neutrons, such as ^{32}Mg and ^{40}Ca , have very different $E(2^+)$ values [163]. (We refer the interested reader to Figures A1-A5 in the appendix for a 2d representation of the data shown in Figures 2 and 3.) The isotopes with magic nucleon numbers have relatively high binding energy, and their charge distribution exhibit smaller variations with respect to the spherical shapes (small quadrupole moments). The nuclear charge radius commonly increases with the number of nucleons, but the slope of the increase is notably smaller approaching the nuclear closed shells. These nuclei are more difficult to excite than their neighbors, which is evidenced by their relatively high excitation energies and low excitation probabilities.

The properties of light nuclei ($A < 20$) are highly sensitive to adding or removing a few nucleons. The lower nuclear orbitals have a smaller degeneracy, thus orbital changes can occur for a few nucleons only. Some particular isotopes, as in the region around $Z = 40$, $N = 60$ and $Z = 62$, $N = 90$, are considered to present a rapid onset of deformation [121, 164]. Interestingly, collective phenomena such as shape coexistence and phase transitions observed for nuclei in the region $Z = 62$, $N = 90$ have been suggested to exhibit analogous features as those for clusters of silicon atoms, which are governed by very different interactions [165].

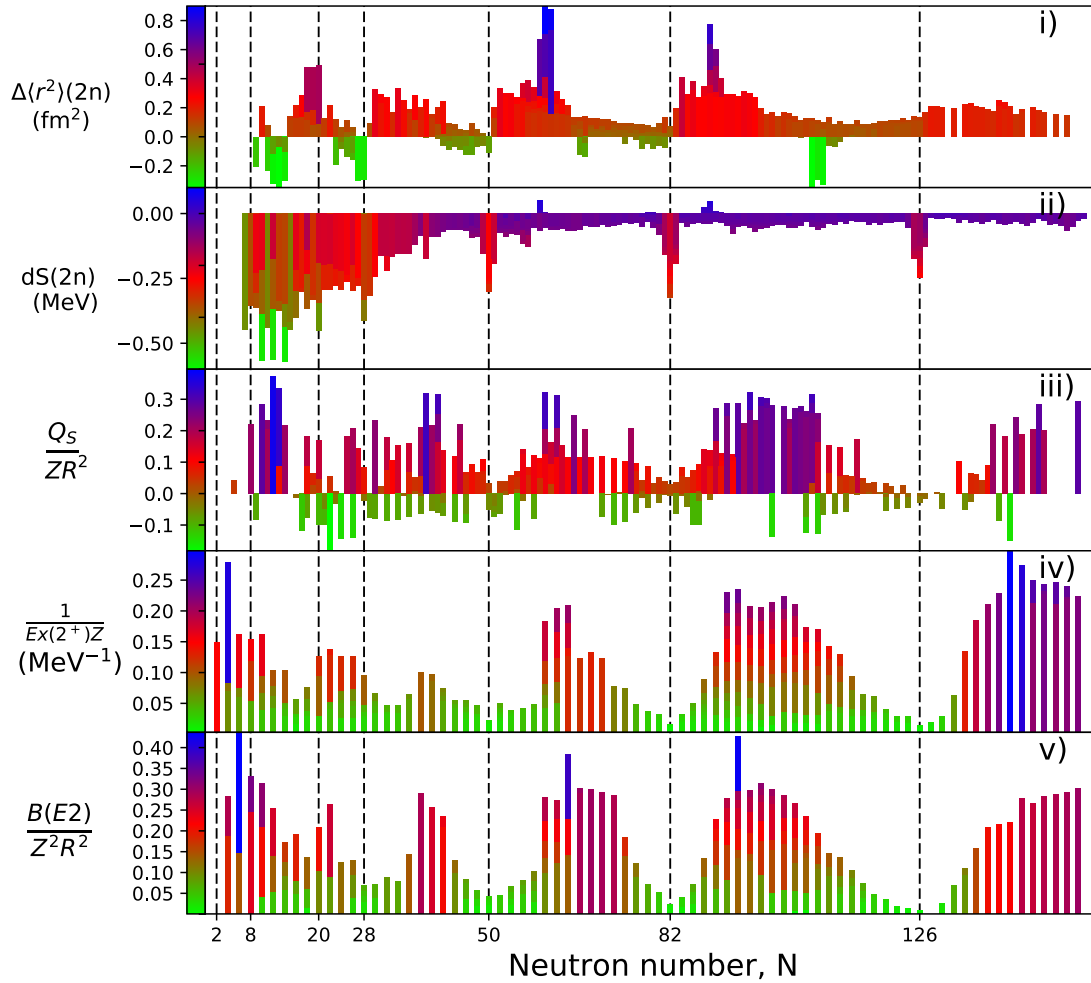


Fig. 2. (Color online) Experimental nuclear properties as a function of the neutron number: i. mean-squared charge radii difference when two neutrons are added, $\langle r^2 \rangle(2n)$; ii. derivative of the two-neutron separation energy dS_{2n} ; iii. normalized spectroscopic quadrupole moments Q_s/ZR^2 ; iv. scaled inverse of the excitation energy of the first 2^+ state, $1/E_{2^+}Z$; and v. normalized transition probability to the first 2^+ excited state, $B(E2)/Z^2R^2$. Data taken from [57–59, 62–64, 123, 135, 138–162].

3.2 Simple patterns in complex nuclei

Nuclear electromagnetic moments such as the magnetic dipole and electric quadrupole moment provide complementary insights into the microscopic and collective properties of nuclei [166, 167]. In fact, electromagnetic moments played a key role in motivating the most basic models of nuclear physics: the nuclear shell model [131], and nuclear deformation [168–170]. Systematic experimental studies of isotopes around nuclear closed shells have revealed surprisingly simple trends in the evolution of nuclear ground-state electromagnetic properties as a function of the neutron number [135, 138–140, 166, 171–173].

Nuclei in the vicinity of the tin isotopes give outstanding examples of simple patterns. The electromagnetic properties of these complex nuclei, with around 50 protons and more than 50 neutrons, seem to be described by a single particle in a nuclear orbital. The experimental nuclear

g -factor (the ratio between the dipole magnetic moment and the nuclear spin) and electric quadrupole moments of cadmium ($Z = 48$), indium ($Z = 49$), and tin ($Z = 50$) isotopes are shown in Figure 4, exhibiting simple trends as a function of neutron number. A simplified single-particle model provides a good description of these observations. In the shell model picture, the electromagnetic properties of odd-even indium isotopes are given by a single proton hole in the $\pi h_{11/2}$ orbit [174–176]. This simple picture of nuclear structure seems to be supported by a rather constant value of their nuclear moments, which present very small variations when neutrons are added. For the even-proton nuclei, cadmium and tin, the naive shell-model expectation is that the electromagnetic properties of even-odd isotopes are dominated by a single neutron occupying the $\nu h_{11/2}$ neutron orbit. This idea is also supported by a constant value of the magnetic moment, and

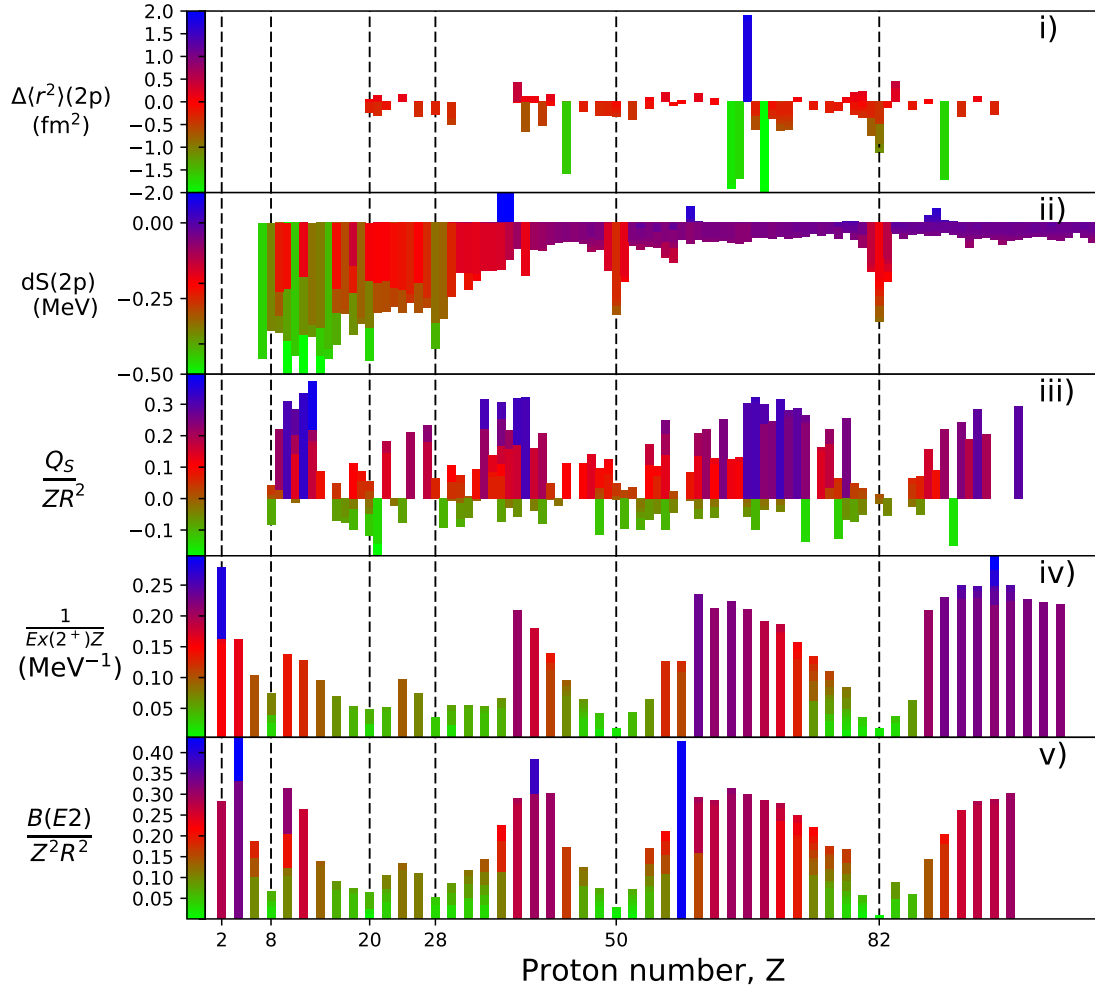


Fig. 3. (Color online) Experimental nuclear properties as a function of the proton number: i. mean-squared charge radii difference when two protons are added, $\langle r^2 \rangle(2p)$; ii. derivative of the two-proton separation energy dS_{2p} ; iii. normalized spectroscopic quadrupole moments Q_s/ZR^2 ; iv. scaled inverse of the excitation energy of the first 2^+ state, $1/E_{2^+}Z$; and v. normalized transition probability to the first 2^+ excited state, $B(E2)/Z^2R^2$. Data taken from [57–59, 62–64, 123, 135, 138–162].

a linear trend in the nuclear quadrupole moments. In this shell model picture, a particle occupying an orbit around closed shells has a negative quadrupole moment, which is interpreted as polarizing a spherical core towards an oblate deformation ($Q_s < 0$) [166]. If neutrons are added to the same orbit, the values of quadrupole moments cross zero when the orbit is half-filled, and take positive values when more than half of the orbit is occupied. This is interpreted as a “hole” polarizing the core towards prolate deformation ($Q_s > 0$). Similar trends have been observed in the calcium ($Z = 20$) [135], nickel ($Z = 28$) [177] and lead ($Z = 82$) [166] regions. Although these trends can be interpreted with phenomenological models, the microscopic origin of these remarkably simple emergent trends are not yet explained from first principles.

3.3 Selected examples for neutron-rich nuclei

Recent developments in both experimental and theoretical tools have provided a deeper insight in our understanding of nuclear properties at extreme proton-to-neutron ratios. Particular interest has been focused on the evolution of nuclear properties towards the suggested neutron-rich doubly magic nuclei: $^{52,54}\text{Ca}$ ($Z = 20$, $N = 32,34$) [123, 136, 137, 143], ^{78}Ni ($Z = 28$, $N = 50$) [145, 146, 178, 179], and ^{132}Sn ($Z = 50$, $N = 82$) [149, 150]. These regions of the nuclear chart are being studied by several experimental techniques providing tests of theoretical descriptions at limits of the nuclear existence. While most of the measured experimental properties (S_{2n} , $E(2^+)$, $B(E2)$, and Q_s) have been described by available nuclear models [135–137, 179, 180], the description of the nuclear size ($\langle r^2 \rangle$) has posed new challenges for modern nuclear theory [123, 150, 151, 181, 182]. This problem has been tackled

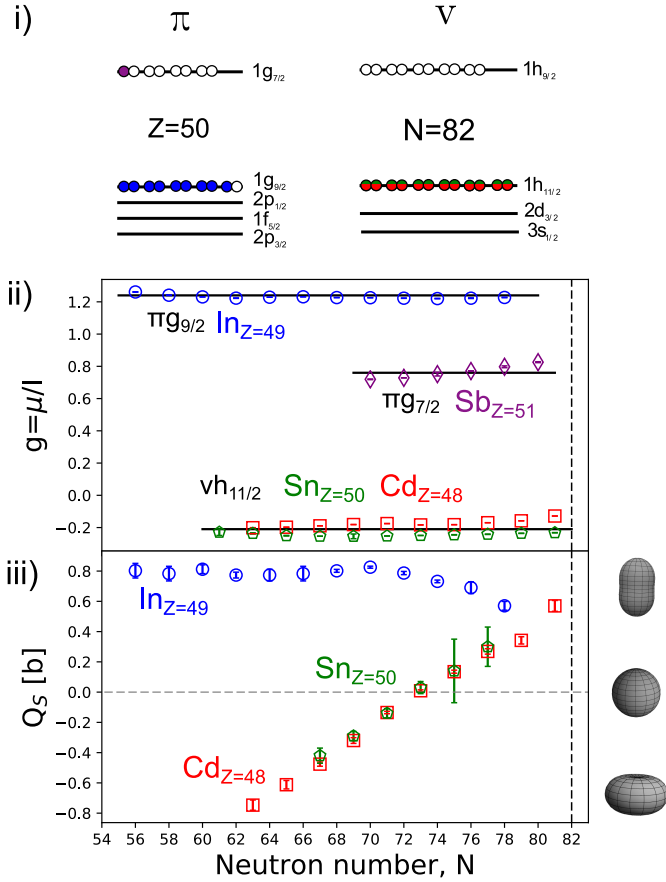


Fig. 4. (Color online) Experimental i) nuclear g -factor and ii) nuclear quadrupole moments of cadmium ($Z = 48$), indium ($Z = 49$), and tin ($Z = 50$) isotopes. The relevant nuclear shell model orbits are shown on the upper panel. Experimental data were taken from [64, 138–142].

with density functional theory, where satisfactory description of charge radii have been obtained in the calcium [151] and tin regions [150]. However, a description in the ab-initio framework has not been achieved yet [123, 182].

Figure 5 shows the changes of the mean-squared charge radii around the calcium, nickel, and tin regions. The values for each isotopic chain are shown with respect to the value at the closed neutron shells. While a strong element dependence is seen close to stability, the charge radii of neutron-rich isotopes beyond the neutron closed-shell appear to increase with surprisingly similar slopes. The radii of the proton-closed-shell calcium isotopes increase as rapid as the open shell isotopes Mn ($Z = 25$) and Fe ($Z = 26$).

Similar charge radii trends have been observed for isotopes around the nickel and tin regions. As illustrated in Figure 5 ii), the nuclear charge radii evolution in the nickel region present a noticeable dependence with the atomic number up to the neutron number $N = 50$. However, for neutron-rich nuclei the mean-squared charge radii of different elements increase with the same slope. Beyond $N = 50$, the radii of isotopes near to the proton closed-

shell such as zinc ($Z = 30$) increase with the same magnitude as the open proton shell isotopes krypton ($Z = 36$) and rubidium ($Z = 37$). These trends are almost identical in the tin region below and beyond the neutron number $N = 82$ (see Figure 5iii).

The rapid increase of the nuclear charge radii observed beyond the neutron number $N = 28$ is in contrast with the patterns seen in isotopes close to stability. For neutron-rich nuclei in the calcium region, the discontinuities seen in other observables such as S_{2n} [136] and $E(2^+)$ [137] values at neutron number $N = 32$, do not appear to be evident in the nuclear charge radii trends. A compilation of different properties measured in the calcium region is shown in Figure 6. The signatures of closed shells at $N = 20$ and $N = 28$ appears across all observables. For the nuclear charge radii (Figure 6i) the signatures at $N = 20$ are present but less pronounced than for $N = 28$. At $N = 32$ and $N = 34$ the clear agreement for the signs of shell closures among the different observables breaks down, and distinct regular patterns appear for different observables.

Only very recently systematic measurements have been achieved for the nuclear charge radii in the vicinity of calcium and tin isotopes beyond $N = 28$ and $N = 82$ [123, 146, 150]. The charge radii and electromagnetic moments of $^{58-70}\text{Ni}$, $^{124-134}\text{Sn}$ and $^{112-134}\text{Sb}$ isotopes have been measured by the COLLAPS collaboration at ISOLDE-CERN [150, 183]. Moreover, results for $^{47-52}\text{K}$ ($Z = 19$), $^{58-78}\text{Cu}$ ($Z = 29$), $^{104-111}\text{Sn}$ ($Z = 50$) and $^{101-131}\text{In}$ ($Z = 49$) isotopes have been obtained by the CRIS collaboration at ISOLDE-CERN [184–187]. Efforts are underway to extend these measurements to more exotic neutron-rich isotopes beyond the ^{52}Ca , ^{132}Sn nuclei [123, 185, 188, 189]. Excitation energy measurements of the doubly-magic shell closure of ^{78}Ni indicates the onset of significant structural changes in neutron-rich isotopes beyond this region [179]. Measurements of the nuclear charge radii of isotopes around $Z = 28$, $N = 50$ and beyond is a challenging area for present experimental studies [186]. The development of radioactive beam facilities [190] and experimental techniques will be required to allow for nuclear charge radii measurements of lighter neutron-rich isotopes in the oxygen region. Their measurement will give insight into the onset of this seemingly nuclear size independent gradient of charge radius increase with neutron number following a shell closure.

4 Conclusions

Despite the drastic difference in the interactions between their constituents, the collective properties of strongly correlated many-body systems exhibit common features. From dust particles governed by Coulomb interactions, atomic clusters interacting by covalent bonds and inter-atomic potentials, up to nuclei governed by short-range nuclear forces. The interactions, length scale and dynamics are very different, but these systems present similar signatures of shell structures and collective phenomena. The commonalities between these many-body systems have shown

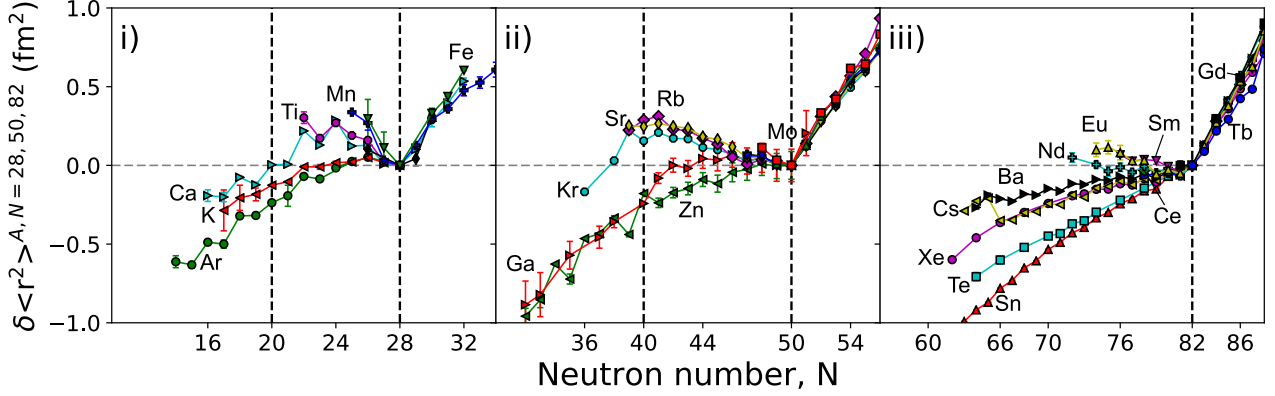


Fig. 5. (Color online) Changes in the mean-square charge radii as a function of the neutron number: i. calcium ($Z = 20$), ii. nickel ($Z = 28$), and iii. tin region ($Z = 50$). Each isotopic chain is shown with respect to the isotope with neutron number at the closed shell. Experimental data were taken from [123,143–152].

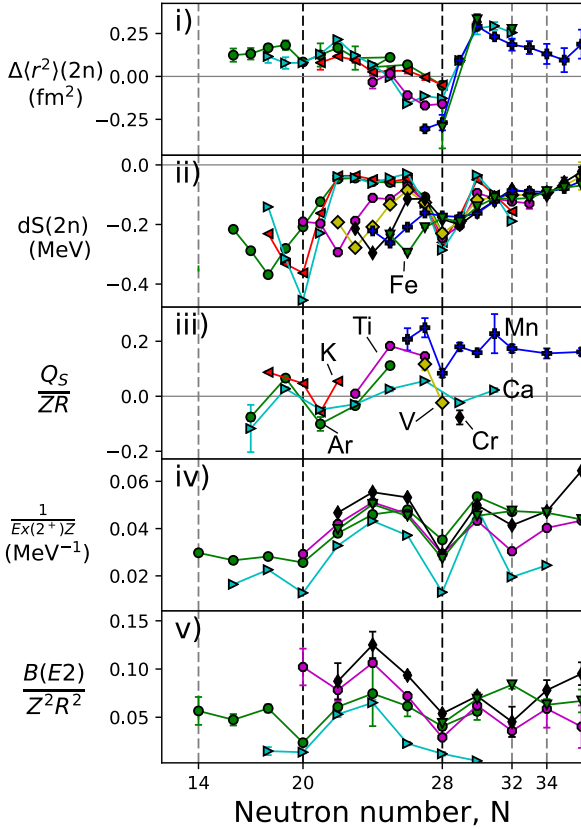


Fig. 6. (Color online) Experimental nuclear properties in the calcium region: i. mean-squared charge radii difference when two neutrons are added, $\langle r^2 \rangle(2n)$; ii. derivative of the two-nucleon separation energy dS_{2n} ; iii. normalized spectroscopic quadrupole moments Q_s/ZR^2 ; iv. scaled inverse of the excitation energy of the first 2^+ state, $1/E_{2^+}Z$; and v. normalized transition probability to the first 2^+ excited state, $B(E2)/Z^2R^2$. Experimental data were taken from [64,123,135,153–162].

to be fruitful to allow for mutual advancements in different fields, as for example was found in the field of atomic nanoclusters by the successful application of modified nuclear structure models. The recent developments in many-body theory and the continuous increase in computing power have allowed an unprecedented reductionist insight of the emergence of physical phenomena. In complex correlated many-body systems, where accurate calculations are particularly challenging, the connection between reductionist and emergence viewpoints is commonly guided through empirical observations. In contrast to other quantum systems, the atomic nucleus is formed by two different constituents (protons and neutrons) that interact mainly by the electromagnetic, strong and weak forces. Moreover, three-body forces appear at a fundamental level in the strong interaction [191].

Recent developments in many-body methods and higher computing power have provided great steps towards the understanding of the microscopic origin of collective phenomena in different regions of the nuclear chart [118,164,192–195]. However, forming a consistent and unified microscopic description of the distinct nuclear phenomena remains as an open problem for nuclear theory. A particular challenge has been the description of nuclear charge radii, where new data in neutron-rich nuclei all exhibit an intriguingly simple increase in charge radii beyond nuclear closed-shells. Moreover, the electromagnetic properties of isotopes around magic numbers of protons and neutrons have been found to exhibit astonishingly simple trends. The microscopic description of these simple patterns, which are predicted by the oldest models of nuclear physics, is a major challenge for modern nuclear theory.

Acknowledgements

This work was supported by ERC Consolidator Grant No.648381 (FNPMML); STFC grants ST/L005794/1, ST/L005786/1, ST/P004423/1 and Ernest Rutherford Grant

No. ST/L002868/1; GOA 15/010 from KU Leuven, BriX Research Program No. P7/12; the FWO-Vlaanderen (Belgium); the European Unions Grant Agreement 654002 (ENSAR2). We thank A. Koszorus and S. Wilkins for helpful comments and suggestions.

Appendix

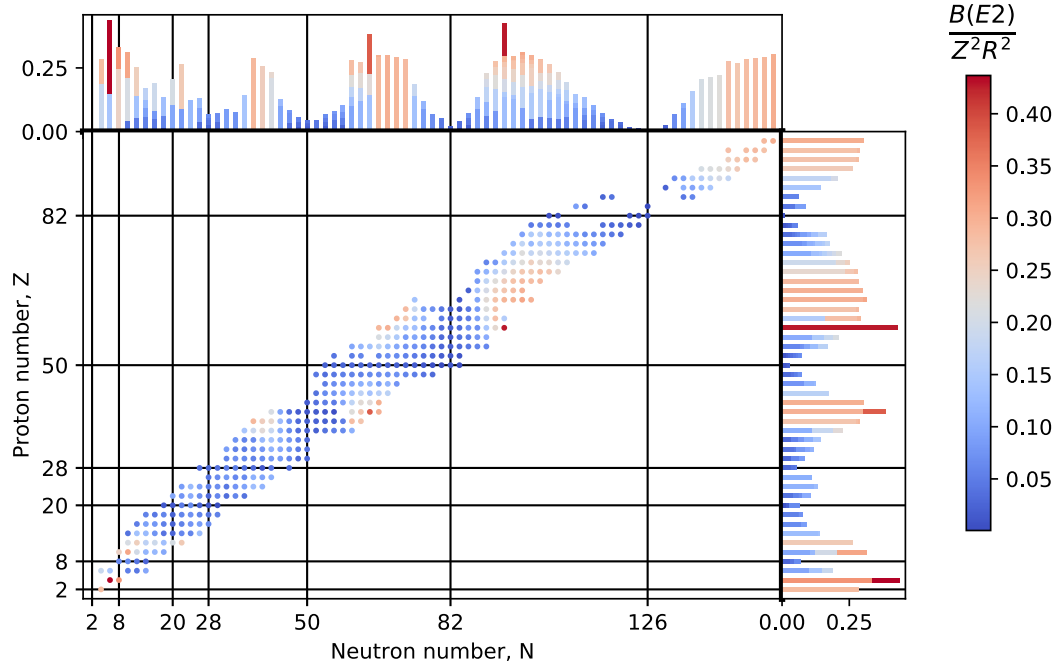


Fig. A1. (Color online) Normalized transition probability to the first 2^+ excited state, $B(E2)/Z^2 R^2$, as a function of the proton number and neutron number. Data taken from [57–59, 62–64, 123, 135, 138–162].

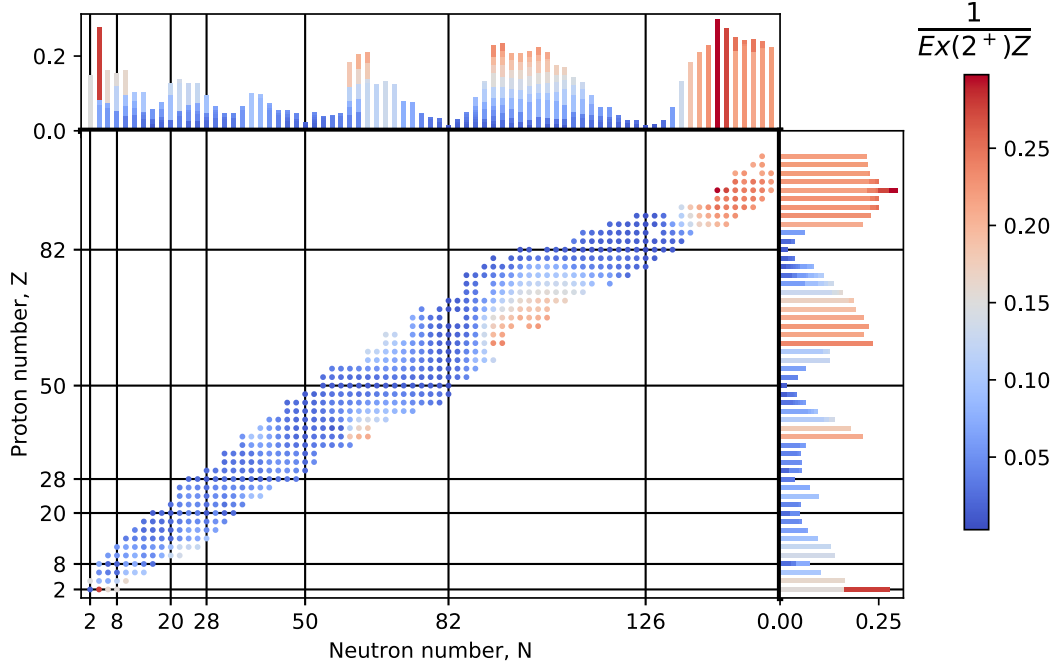


Fig. A2. (Color online) Scaled inverse of the excitation energy of the first 2^+ state, $1/E_{2^+}Z$, as a function of the proton number and neutron number. Data taken from [57–59, 62–64, 123, 135, 138–162].

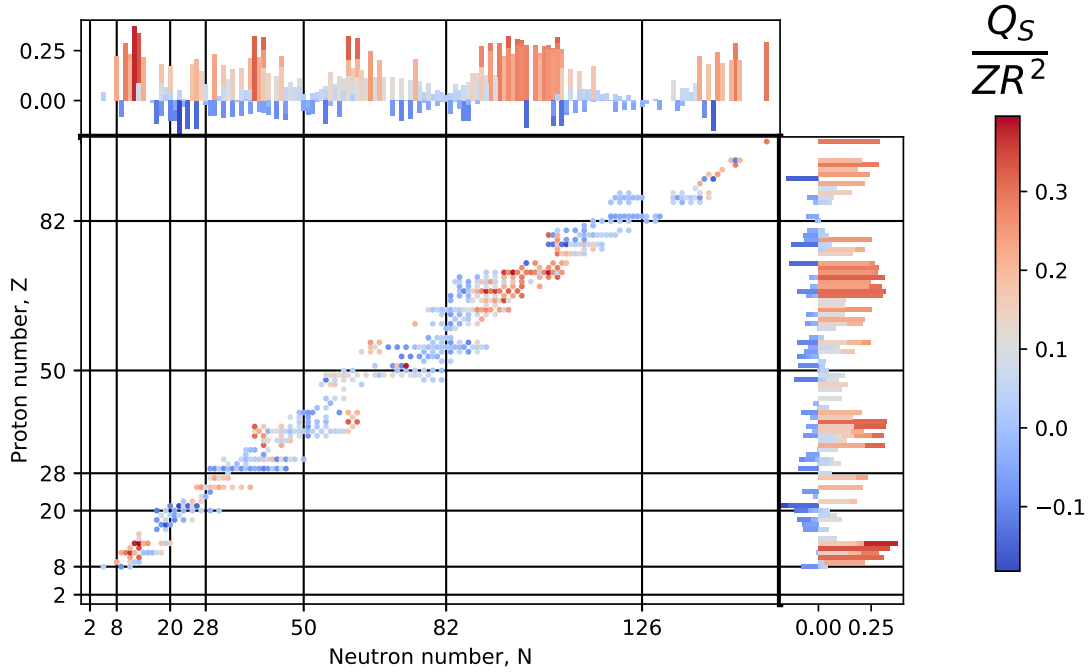


Fig. A3. (Color online) Normalized spectroscopic quadrupole moments Q_s/ZR^2 , as a function of the proton number and neutron number. Data taken from [57–59, 62–64, 123, 135, 138–162].

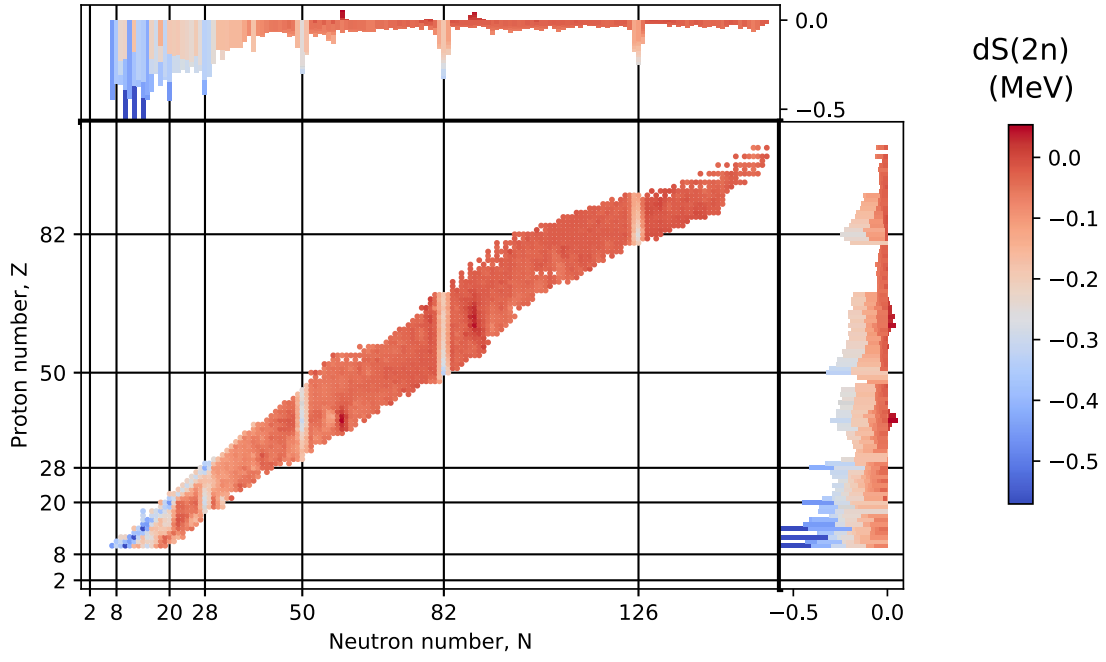


Fig. A4. (Color online) Derivative of the two-proton separation energy dS_{2n} , as a function of the proton number and neutron number. Data taken from [57–59, 62–64, 123, 135, 138–162].

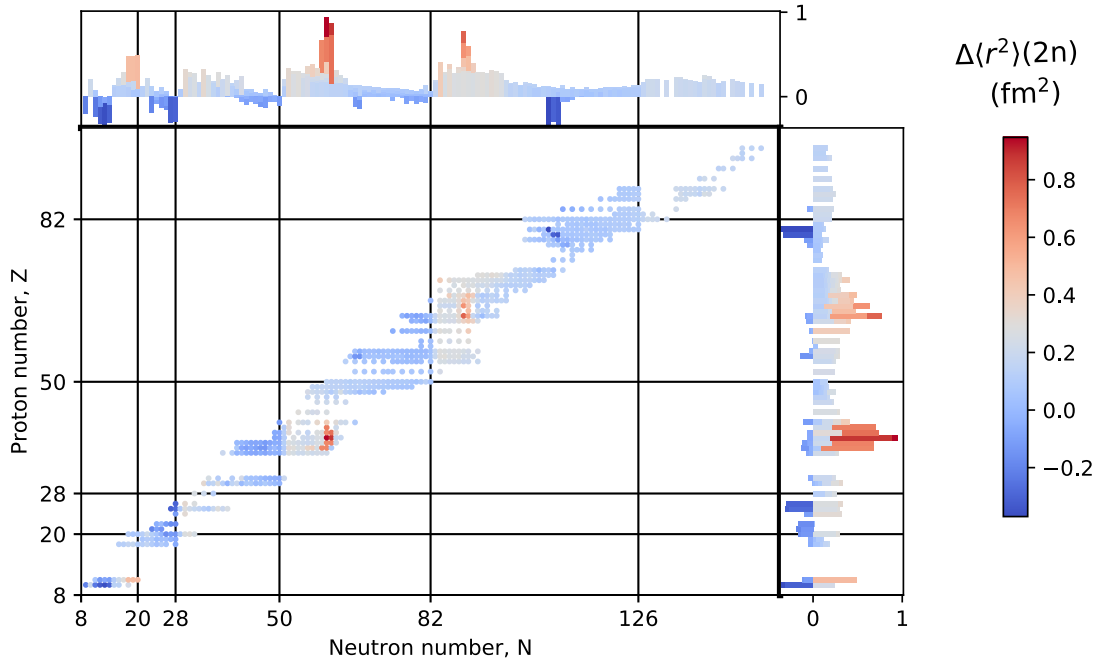


Fig. A5. (Color online) Mean-squared charge radii difference when two protons are added, $\langle r^2 \rangle(2n)$, as a function of the proton number and neutron number. Data taken from [57–59, 62–64, 123, 135, 138–162].

References

- Erin G Teich, Greg van Anders, Daphne Klotsa, Julia Dshemuchadse, and Sharon C Glotzer. Clusters of polyhedra in spherical confinement. *Proceedings of the National Academy of Sciences of the United States of America*, 113(6):E669–78, feb 2016.
- Didier Reinhardt. Phyllotaxis - A new chapter in an old tale about beauty and magic numbers. *Current Opinion in Plant Biology*, 8(5):487–493, oct 2005.
- Oliver Arp, Dietmar Block, Alexander Piel, and André Melzer. Dust coulomb balls: Three-dimensional plasma crystals. *Physical Review Letters*, 93(16), oct 2004.
- I. V. Grigorieva, W. Escoffier, J. Richardson, L. Y. Vinnikov, S. Dubonos, and V. Oboznov. Direct observation of vortex shells and magic numbers in mesoscopic superconducting disks. *Physical Review Letters*, 96(7), 2006.
- Junwei Wang, Chrameh Fru Mbah, Thomas Przybilla, Benjamin Apeleo Zubiri, Erdmann Spiecker, Michael Engel, and Nicolas Vogel. Magic number colloidal clusters as minimum free energy structures. *Nature Communications*, 9(1), dec 2018.
- Hans E. Suess and Harold C. Urey. Abundances of the Elements. *Reviews of Modern Physics*, 28(1):53–74, jan 1956.
- Patrick W. Fowler and David E. Manolopoulos. Magic numbers and stable structures for fullerenes, fullerides and fullerenium ions. *Nature*, 355(6359):428–430, 1992.
- Matthias Brack. The physics of simple metal clusters: Self-consistent jellium model and semiclassical approaches. *Reviews of Modern Physics*, 65(3):677–732, 1993.
- Walt A. De Heer. The physics of simple metal clusters: Experimental aspects and simple models. *Reviews of Modern Physics*, 65(3):611–676, 1993.
- P. W. Anderson. More Is Different. *Science*, 177(4047):393–396, aug 1972.
- Michael Schmidt and Hod Lipson. Distilling Free-Form Natural Laws from Experimental Data. *Science*, 324(5923):81–85, 2009.
- Nigel Goldenfeld and Leo P Kadanoff. Simple Lessons from Complexity. *Science*, 284(5411):87–89, 1999.
- Igal Talmi. *Simple Models of Complex Nuclei*. Routledge, 1993.
- Sophie C. Gibb, Robin Findlay Hendry, and Tom Lancaster. *The Routledge Handbook of Philosophy of Emergence*. Routledge, 2018.
- Piers Coleman. Emergence and Reductionism: an awkward Baconian alliance. *arXiv*, 1702.06884, feb 2017.
- National Museum of Mathematics. Sunflower Seed Pattern.
- Thomas Splettstößer. File:Adenovirus 3D schematic.png, 2019.
- Rob Hooft. File:C60-rods.png, 2019.
- Matthias Brack. Metal Clusters and Magic Numbers. *Scientific American*, 277(6):50–55, 1997.
- File:Atomic-orbital-clouds spdf m0.png, 2019.
- J.N. Ridley. Packing efficiency in sunflower heads. *Mathematical Biosciences*, 58(1):129–139, feb 1982.
- Helmut Vogel. A better way to construct the sunflower head. *Mathematical Biosciences*, 44(3-4):179–189, jun 1979.
- W. Krätschmer, Lowell D. Lamb, K. Fostiropoulos, and Donald R. Huffman. Solid C60: a new form of carbon. *Nature*, 347(6291):354–358, 1990.
- François Diederich, Roland Ettl, Yves Rubin, Robert L. Whetten, Rainer Beck, Marcos Alvarez, Samir Anz, Dilip Sensharma, Fred Wudl, Kishan C. Khemani, and Andrew Koch. The higher fullerenes: Isolation and characterization of C76, C84, C90, C94, and C70O, an oxide of D5h-C70. *Science*, 252(5005):548–551, 1991.
- O. Echt, K. Sattler, and E. Recknagel. Magic Numbers for Sphere Packings: Experimental Verification in Free Xenon Clusters. *Physical Review Letters*, 47(16):1121–1124, oct 1981.
- O. Echt, M. C. Cook, and A. W. Castleman. Multiphoton ionization studies of xenon clusters. *Chemical Physics Letters*, 135(3):229–235, apr 1987.
- W. D. Knight, Keith Clemenger, Walt A. de Heer, Winston A. Saunders, M. Y. Chou, and Marvin L. Cohen. Electronic Shell Structure and Abundances of Sodium Clusters. *Physical Review Letters*, 52(24):2141–2143, jun 1984.
- J. Pedersen, S. Bjørnholm, J. Borggreen, K. Hansen, T. P. Martin, and H. D. Rasmussen. Observation of quantum supershells in clusters of sodium atoms. *Nature*, 353(6346):733–735, 1991.
- Hellmut Haberland, Thomas Hippler, Jörn Donges, Oleg Kostko, Martin Schmidt, and Bernd Von Issendorff. Melting of sodium clusters: Where do the magic numbers come from? *Physical Review Letters*, 94(3), jan 2005.
- Duncan E.K. Sutherland and Martin J. Stillman. The "magic numbers" of metallothionein. *Metallomics*, 3(5):444–463, may 2011.
- D. Marenduzzo, C. Micheletti, and E. Orlandini. Biopolymer organization upon confinement. *Journal of Physics Condensed Matter*, 22(28), jul 2010.
- R. John Ellis. Macromolecular crowding: Obvious but underappreciated. *Trends in Biochemical Sciences*, 26(10):597–604, oct 2001.
- A M Turing. The Chemical Basis of Morphogenesis. *Philosophical Transactions of the Royal Society of London. Series B, Biological Sciences*, 237(641):37–72, 1952.
- Hajar Vakili, Pavel Kroupa, and Sohrab Rahvar. Type I Shell Galaxies as a Test of Gravity Models. *The Astrophysical Journal*, 848(1):55, oct 2017.
- Douglas B. Cines, Tatiana Lebedeva, Chandrasekaran Nagaswami, Vincent Hayes, Walter Massefski, Rustem I. Litvinov, Lubica Rauova, Thomas J. Lowery, and John W. Weisel. Clot contraction: Compression of erythrocytes into tightly packed polyhedra and redistribution of platelets and fibrin. *Blood*, 123(10):1596–1603, mar 2014.
- Takashi Hayashi and Richard W. Carthew. Surface mechanics mediate pattern formation in the developing retina. *Nature*, 431(7009):647–652, oct 2004.
- J. A.S. Kelso and G. Schöner. Self-organization of coordinative movement patterns. *Human Movement Science*, 7(1):27–46, 1988.
- G. Schöner and J. A.S. Kelso. Dynamic pattern generation in behavioral and neural systems. *Science*, 239(4847):1513–1520, 1988.
- G. J. Mitchison. Phyllotaxis and the fibonacci series. *Science*, 196(4287):270–275, 1977.

40. Didier Reinhardt, Eva Rachele Pesce, Pia Stieger, Therese Mandel, Kurt Baltensperger, Malcolm Bennett, Jan Traas, Jiří Friml, and Cris Kuhlemeier. Regulation of phyllotaxis by polar auxin transport. *Nature*, 426(6964):255–260, nov 2003.
41. Reza Farhadifar, Jens Christian Röper, Benoit Aigouy, Suzanne Eaton, and Frank Jülicher. The Influence of Cell Mechanics, Cell-Cell Interactions, and Proliferation on Epithelial Packing. *Current Biology*, 17(24):2095–2104, dec 2007.
42. Hiroaki Ohfuji and David Rickard. Experimental syntheses of frambooids - A review. *Earth-Science Reviews*, 71(3-4):147–170, aug 2005.
43. Hiroaki Ohfuji and Junji Akai. Icosahedral domain structure of frambooidal pyrite. *American Mineralogist*, 87(1):176–180, 2002.
44. S. Elizabeth Norred, Patrick M. Caveney, Gaurav Chauhan, Lauren K. Collier, C. Patrick Collier, Steven M. Abel, and Michael L. Simpson. Macromolecular Crowding Induces Spatial Correlations That Control Gene Expression Bursting Patterns. *ACS Synthetic Biology*, 7(5):1251–1258, may 2018.
45. R. John Ellis and Allen P. Minton. Join the crowd. *Nature*, 425(6953):27–28, sep 2003.
46. Cristian Micheletti, Davide Marenduzzo, and Enzo Orlandini. Polymers with spatial or topological constraints: Theoretical and computational results. *Physics Reports*, 504(1):1–73, jul 2011.
47. S. Tarucha, D. G. Austing, T. Honda, R. J. van der Hage, and L. P. Kouwenhoven. Shell filling and spin effects in a few electron quantum dot. *Physical Review Letters*, 77(17):3613–3616, 1996.
48. Mauricio G. Mateu. Assembly, stability and dynamics of virus capsids, mar 2013.
49. Antoni Luque, Roya Zandi, and David Reguera. Optimal architectures of elongated viruses. *Proceedings of the National Academy of Sciences of the United States of America*, 107(12):5323–5328, mar 2010.
50. Ting Chen and Sharon C. Glotzer. Simulation studies of a phenomenological model for elongated virus capsid formation. *Physical Review E - Statistical, Nonlinear, and Soft Matter Physics*, 75(5), may 2007.
51. W. H. Roos, R. Bruinsma, and G. J.L. Wuite. Physical virology. *Nature Physics*, 6(10):733–743, 2010.
52. Bonnie Berger, Peter W. Shor, Lisa Tucker-Kellogg, and Jonathan King. Local rule-based theory of virus shell assembly. *Proceedings of the National Academy of Sciences of the United States of America*, 91(16):7732–7736, aug 1994.
53. Anish Goel, Jack B. Howard, and John B. Vander Sande. Size analysis of single fullerene molecules by electron microscopy. *Carbon*, 42(10):1907–1915, jan 2004.
54. Han Myoung Lee, Seung Bum Suh, P. Tarakeshwar, and Kwang S. Kim. Origin of the magic numbers of water clusters with an excess electron. *Journal of Chemical Physics*, 122(4), 2005.
55. M. L. Homer, J. L. Persson, E. C. Honea, and R. L. Whetten. Ionization energies and stabilities of Nan, n₂5: shell structure from measurements on cold clusters. *Zeitschrift für Physik D Atoms, Molecules and Clusters*, 22(1):441–447, mar 1991.
56. NIST ASD Team A. Kramida, Y. Ralchenko, J. Reader. NIST Atomic Spectra Database, 2019.
57. G Audi, Meng Wang, A H Wapstra, G Audi, F G Kondev, W J Huang, S Naimi, and Xing Xu. Chinese Physics C. *Chinese Physics C*, 41(3):30003, 2017.
58. Meng Wang, G. Audi, F. G. Kondev, W.J. J Huang, S. Naimi, and Xing Xu. The AME2016 atomic mass evaluation (II). Tables, graphs and references. *Chinese Physics C*, 41(3):30003, mar 2017.
59. G. Audi, F. G. Kondev, Meng Wang, W. J. Huang, and S. Naimi. The NUBASE2016 evaluation of nuclear properties. *Chinese Physics C*, 41(3), mar 2017.
60. L. W. Nordheim. β -Decay and the nuclear shell model. *Physical Review*, 78(3):294, 1950.
61. M. Ismail, W. M. Seif, and A. Abdurrahman. Relative stability and magic numbers of nuclei deduced from behavior of cluster emission half-lives. *Physical Review C*, 94(2), aug 2016.
62. I. Angeli and K.P. Marinova. Table of experimental nuclear ground state charge radii: An update. *Atomic Data and Nuclear Data Tables*, 99(1):69–95, jan 2013.
63. B. Pritychenko, M. Birch, B. Singh, and M. Horoi. Tables of E2 transition probabilities from the first 2+ states in even-even nuclei. *Atomic Data and Nuclear Data Tables*, 107:1–139, jan 2016.
64. N. J. Stone. Table of nuclear electric quadrupole moments. *Atomic Data and Nuclear Data Tables*, 111-112:1–28, sep 2016.
65. N. Grevesse and A.J. Sauval. Standard Solar Composition. *Space Science Reviews*, 85(1/2):161–174, 1998.
66. H. Hurwitz and H. A. Bethe. Neutron capture cross sections and level density, 1951.
67. Ralph A. Alpher and Robert C. Herman. Theory of the origin and relative abundance distribution of the elements. *Reviews of Modern Physics*, 22(2):153–212, 1950.
68. Edward Anders and Nicolas Grevesse. Abundances of the elements: Meteoritic and solar. *Geochimica et Cosmochimica Acta*, 53(1):197–214, 1989.
69. B. E. J. Pagel. *Nucleosynthesis and chemical evolution of galaxies*. Cambridge University Press, 2009.
70. Michael A. Boles, Michael Engel, and Dmitri V. Talapin. Self-assembly of colloidal nanocrystals: From intricate structures to functional materials. *Chemical Reviews*, 116(18):11220–11289, sep 2016.
71. R. Rutgers. Packing of spheres. *Nature*, 193(4814):465–466, 1962.
72. Ignacio Castillo, Frank J. Kampas, and János D. Pintér. Solving circle packing problems by global optimization: Numerical results and industrial applications. *European Journal of Operational Research*, 191(3):786–802, dec 2008.
73. Maria Goepfert Mayer. On Closed Shells in Nuclei. II. *Physical Review*, 75(12):1969–1970, jun 1949.
74. Otto Haxel, J. Hans D. Jensen, and Hans E. Suess. On the "magic numbers" in nuclear structure, 1949.
75. M. Bonitz, C. Henning, and D. Block. Complex plasmas: A laboratory for strong correlations. *Reports on Progress in Physics*, 73(6), 2010.
76. V. E. Fortov, A. V. Ivlev, S. A. Khrapak, A. G. Khrapak, and G. E. Morfill. Complex (dusty) plasmas: Current status, open issues, perspectives. *Physics Reports*, 421(1-2):1–103, dec 2005.
77. O Arp, D Block, M Bonitz, H Fehske, V Golubnychiy, S Kosse, P Ludwig, A Melzer, and A Piel. 3D Coulomb balls: experiment and simulation. *Journal of Physics: Conference Series*, 11:234–247, jan 2005.

78. O. Arp, D. Block, M. Klindworth, and A. Piel. Confinement of Coulomb balls. *Physics of Plasmas*, 12(12):1–9, 2005.
79. P. Ludwig, S. Kosse, and M. Bonitz. Structure of spherical three-dimensional Coulomb crystals. *Physical Review E - Statistical, Nonlinear, and Soft Matter Physics*, 71(4), apr 2005.
80. Wen Tau Juan, Zen Hong Huang, Ju Wang Hsu, Yin Ju Lai, and I. Lin. Observation of dust Coulomb clusters in a plasma trap. *Physical Review E*, 58(6):R6947–R6950, 1998.
81. A. D. Dinsmore, Ming F. Hsu, M. G. Nikolaides, Manuel Marquez, A. R. Bausch, and D. A. Weitz. Colloidosomes: Selectively permeable capsules composed of colloidal particles. *Science*, 298(5595):1006–1009, nov 2002.
82. Bart De Nijs, Simone Dussi, Frank Smalenburg, Johannes D. Meeldijk, Dirk J. Groenendijk, Laura Filion, Arnout Imhof, Alfons Van Blaaderen, and Marjolein Dijkstra. Entropy-driven formation of large icosahedral colloidal clusters by spherical confinement. *Nature Materials*, 14(1):56–60, jan 2015.
83. Thomas Kister, Marko Mravljak, Tanja Schilling, and Tobias Kraus. Pressure-controlled formation of crystalline, Janus, and core-shell supraparticles. *Nanoscale*, 8(27):13377–13384, jul 2016.
84. Vinodhan N. Manoharan, Mark T. Elsesser, and David J. Pine. Dense packing and symmetry in small clusters of microspheres. *Science*, 301(5632):483–487, jul 2003.
85. Guangnan Meng, Natalie Arkus, Michael P. Brenner, and Vinodhan N. Manoharan. The free-energy landscape of clusters of attractive hard spheres. *Science*, 327(5965):560–563, 2010.
86. Noel A. Clark, Alan J. Hurd, and Bruce J. Ackerson. Single colloidal crystals. *Nature*, 281(5726):57–60, 1979.
87. Orlin D. Velev, Abraham M. Lenhoff, and Eric W. Kaler. A class of microstructured particles through colloidal crystallization. *Science*, 287(5461):2240–2243, mar 2000.
88. T.P. Martin. Shells of atoms. *Physics Reports*, 273(4):199–241, aug 1996.
89. Marvin L. Cohen and Walter D. Knight. The Physics of Metal Clusters. *Physics Today*, 43(12):42–50, dec 1990.
90. H. Nishioka, Klavs Hansen, and B. R. Mottelson. Super-shells in metal clusters. *Physical Review B*, 42(15):9377–9386, 1990.
91. I. Katakuse, T. Ichihara, Y. Fujita, T. Matsuo, T. Sakurai, and H. Matsuda. Mass distributions of copper, silver and gold clusters and electronic shell structure. *International Journal of Mass Spectrometry and Ion Processes*, 67(2):229–236, nov 1985.
92. W. Ekardt. Work function of small metal particles: Self-consistent spherical jellium-background model. *Physical Review B*, 29(4):1558–1564, feb 1984.
93. Jia Jie Li, Wen Hui Long, Jérôme Margueron, and Nguyen Van Giai. Superheavy magic structures in the relativistic Hartree-Fock-Bogoliubov approach. *Physics Letters, Section B: Nuclear, Elementary Particle and High-Energy Physics*, 732:169–173, may 2014.
94. Mark A. Stoyer. Island ahoy! *Nature*, 442(7105):876–877, aug 2006.
95. S.G. Nilsson. Binding states of individual nucleons in strongly deformed nuclei. *Kong.Dan. Vid.Sel.Mat.Fys.Med.*, 29N16:1–69, 1955.
96. Keith Clemenger. Ellipsoidal shell structure in free-electron metal clusters. *Physical Review B*, 32(2):1359–1362, jul 1985.
97. B. L. Berman and S. C. Fultz. Measurements of the giant dipole resonance with monoenergetic photons. *Reviews of Modern Physics*, 47(3):713–761, jul 1975.
98. W. Ekardt. Collective multipole excitations in small metal particles: Critical angular momentum for the existence of collective surface modes. *Physical Review B*, 32(4):1961–1970, aug 1985.
99. Søren Raza, Shima Kadkhodazadeh, Thomas Christensen, Marcel Di Vece, Martijn Wubs, N. Asger Mortensen, and Nicolas Stenger. Multipole plasmons and their disappearance in few-nanometre silver nanoparticles. *Nature Communications*, 6(1):8788, dec 2015.
100. Eric C. Honea, Margie L. Homer, John L. Persson, and Robert L. Whetten. Generation and photoionization of cold Nan clusters; n to 200. *Chemical Physics Letters*, 171(3):147–154, aug 1990.
101. M. P. Iñiguez, J. A. Alonso, and L. C. Balbas. Magic numbers of sodium clusters. *Solid State Communications*, 57(1):85–88, 1986.
102. G. Wrigge, M. Astruc Hoffmann, and B. V. Issendorff. Photoelectron spectroscopy of sodium clusters: Direct observation of the electronic shell structure. *Physical Review A - Atomic, Molecular, and Optical Physics*, 65(6):5, 2002.
103. M. Schmidt, J. Donges, Th Hippler, and H. Haberland. Influence of Energy and Entropy on the Melting of Sodium Clusters. *Physical Review Letters*, 90(10):4, mar 2003.
104. Joachim Alexander Maruhn, Paul Gerhard Reinhard, and Eric Suraud. *Simple models of many-fermion systems*. Springer Berlin Heidelberg, 2010.
105. Mary K. Gaillard, Paul D. Grannis, and Frank J. Sciulli. The standard model of particle physics. *Reviews of Modern Physics*, 71(2):S96–S111, mar 1999.
106. C.J. Foot. *Atomic Physics*, volume 25. OUP Oxford, 2004.
107. J. Bardeen, L. N. Cooper, and J. R. Schrieffer. Theory of superconductivity. *Physical Review*, 108(5):1175–1204, 1957.
108. Guido Altarelli. The Standard Model of Particle Physics. *arXiv preprint*, oct 2005.
109. L. F. Pašteka, E. Eliav, A. Borschevsky, U. Kaldor, and P. Schwerdtfeger. Relativistic Coupled Cluster Calculations with Variational Quantum Electrodynamics Resolve the Discrepancy between Experiment and Theory Concerning the Electron Affinity and Ionization Potential of Gold. *Physical Review Letters*, 118(2), jan 2017.
110. Ephraim Eliav, Anastasia Borschevsky, and Uzi Kaldor. High-Accuracy Relativistic Coupled Cluster Calculations for the Heaviest Elements. In *Handbook of Relativistic Quantum Chemistry*, pages 1–31. Springer Berlin Heidelberg, 2015.
111. Krzysztof Pachucki. Improved theory of helium fine structure. *Physical Review Letters*, 97(1), 2006.
112. Krzysztof Pachucki and Jacek Komasa. Relativistic and QED corrections for the beryllium atom. *Physical Review Letters*, 92(21), may 2004.
113. Vladimir Korobov and Alexander Yelkhovsky. Ionization potential of the helium atom. *Physical Review Letters*, 87(19):193003, oct 2001.

114. Emmanuel Chang, Zohreh Davoudi, William Detmold, Arjun S. Gambhir, Kostas Orginos, Martin J. Savage, Phiala E. Shanahan, Michael L. Wagman, and Frank Winter. Scalar, Axial, and Tensor Interactions of Light Nuclei from Lattice QCD. *Physical Review Letters*, 120(15), apr 2018.
115. A. Gezerlis, I. Tews, E. Epelbaum, S. Gandolfi, K. Hebeler, A. Nogga, and A. Schwenk. Quantum Monte Carlo calculations with chiral effective field theory interactions. *Physical Review Letters*, 111(3), jul 2013.
116. N. Barnea, L. Contessi, D. Gazit, F. Pederiva, and U. Van Kolck. Effective field theory for lattice nuclei. *Physical Review Letters*, 114(5), feb 2015.
117. E. Epelbaum, H. W. Hammer, and Ulf G. Meißner. Modern theory of nuclear forces. *Reviews of Modern Physics*, 81(4):1773–1825, dec 2009.
118. T Otsuka, Y Tsunoda, T Abe, N Shimizu, and P Van Duppen. Underlying structure of collective bands and self-organization in quantum systems. *Physical Review Letters*, Accepted, 2019.
119. T. Dytrych, K. D. Launey, J. P. Draayer, D. J. Rowe, J. L. Wood, G. Rosensteel, C. Bahri, D. Langr, and R. B. Baker. Physics of Nuclei: Key Role of an Emergent Symmetry. *Physical Review Letters*, 124(4):042501, jan 2020.
120. Hans-Werner Hammer, Andreas Nogga, and Achim Schwenk. π Colloquium: Three-body forces: From cold atoms to nuclei. *Reviews of Modern Physics*, 85(1):197–217, 2013.
121. Kris Heyde and John L Wood. Shape coexistence in atomic nuclei. *Rev. Mod. Phys.*, 83(4):1467–1521, nov 2011.
122. Z. T. Lu, P. Mueller, G. W.F. Drake, W. Nörtershäuser, Steven C. Pieper, and Z. C. Yan. Colloquium: Laser probing of neutron-rich nuclei in light atoms. *Reviews of Modern Physics*, 85(4):1383–1400, oct 2013.
123. R. F. Garcia Ruiz, M. L. Bissell, K. Blaum, A. Ekström, N. Frömmgen, G. Hagen, M. Hammen, K. Hebeler, J. D. Holt, G. R. Jansen, M. Kowalska, K. Kreim, W. Nazarewicz, R. Neugart, G. Neyens, W. Nörtershäuser, T. Papenbrock, J. Papuga, A. Schwenk, J. Simonis, K. A. A. Wendt, and D. T. Yordanov. Unexpectedly large charge radii of neutron-rich calcium isotopes. *Nature Physics*, 12(6):594–598, jun 2016.
124. Martin Freer, Hisashi Horiuchi, Yoshiko Kanada-En'yo, Dean Lee, and Ulf-G. Meißner. Microscopic clustering in light nuclei. *Reviews of Modern Physics*, 90(3):035004, aug 2018.
125. J A S Smith. Nuclear quadrupole interactions in solids. *Chem. Soc. Rev.*, 15(2):225–260, 1986.
126. R F Casten, N V Zamfir, and D S Brenner. Universal anharmonic vibrator description of nuclei and critical nuclear phase transitions. *Phys. Rev. Lett.*, 71(2):227–230, jul 1993.
127. O. Sorlin and M. G. Porquet. Nuclear magic numbers: New features far from stability. *Progress in Particle and Nuclear Physics*, 61(2):602–673, oct 2008.
128. I Angeli and K P Marinova. Correlations of nuclear charge radii with other nuclear observables. *Journal of Physics G: Nuclear and Particle Physics*, 42(5):55108, mar 2015.
129. I. Bentley, Y. Colón Rodríguez, S. Cunningham, and A. Aprahamian. Shell structure from nuclear observables. *Physical Review C*, 93(4):044337, apr 2016.
130. R F Casten. Symmetries and regularities in nuclei: Order out of seeming chaos. *AIP Conference Proceedings*, 2150:20001, 2019.
131. Maria Goeppert Mayer. Nuclear Configurations in the Spin-Orbit Coupling Model. I. Empirical Evidence. *Physical Review*, 78(1):16–21, apr 1950.
132. Maria Goeppert Mayer. Nuclear Configurations in the Spin-Orbit Coupling Model. II. Theoretical Considerations. *Phys. Rev.*, 78(1):22–23, apr 1950.
133. A Bohr and B R Mottelson. *Nuclear Structure*, volume I and II. Benjamin, New York, 1975.
134. R B Cakirli, R F Casten, and K Blaum. Correlations of experimental isotope shifts with spectroscopic and mass observables. *Phys. Rev. C*, 82(6):61306, dec 2010.
135. R. F. Garcia Ruiz, M. L. Bissell, K. Blaum, N. Frömmgen, M. Hammen, J. D. Holt, M. Kowalska, K. Kreim, J. Menéndez, R. Neugart, G. Neyens, W. Nörtershäuser, F. Nowacki, J. Papuga, A. Poves, A. Schwenk, J. Simonis, D. T. Yordanov, R. F. Garcia Ruiz, M. L. Bissell, K. Blaum, N. Frömmgen, M. Hammen, J. D. Holt, M. Kowalska, K. Kreim, J. Menéndez, R. Neugart, G. Neyens, W. Nörtershäuser, F. Nowacki, J. Papuga, A. Poves, A. Schwenk, J. Simonis, and D. T. Yordanov. Ground-state electromagnetic moments of calcium isotopes. *Physical Review C*, 91(4):041304, apr 2015.
136. F. Wienholtz, D. Beck, K. Blaum, Ch Borgmann, M. Breitenfeldt, R. B. Cakirli, S. George, F. Herfurth, J. D. Holt, M. Kowalska, S. Kreim, D. Lunney, V. Manea, J. Menéndez, D. Neidherr, M. Rosenbusch, L. Schweikhard, A. Schwenk, J. Simonis, J. Stanja, R. N. Wolf, and K. Zuber. Masses of exotic calcium isotopes pin down nuclear forces. *Nature*, 498(7454):346–349, jun 2013.
137. D Steppenbeck Et al. Evidence for a new nuclear magic number' from the level structure of ^{54}Ca . *Nature*, 502:207, 2013.
138. J. Eberz, U. Dinger, G. Huber, H. Lochmann, R. Menges, R. Neugart, R. Kirchner, O. Klepper, T. Köhl, D. Marx, G. Ulm, and K. Wendt. Spins, moments and mean square charge radii of $^{104-127}\text{In}$ determined by laser spectroscopy. *Nuclear Physics A*, 464(1):9–28, mar 1987.
139. F Le Blanc, L Cabaret, E Cottureau, J E Crawford, S Essabaa, J Genevey, R Horn, G Huber, J Lassen, J K P Lee, G Le Scornet, J Obert, J Oms, A Ouchrif, J Pinard, B Roussie're, J Sauvage, and D Verney. Charge radii and nuclear moments around ^{132}Sn . *Nuclear Physics A*, 734:437–440, 2004.
140. D T Yordanov, D L Balabanski, M L Bissell, K Blaum, S Fritzsche, N Frömmgen, G Georgiev, Ch. Geppert, M Hammen, M Kowalska, K Kreim, A Krieger, R Neugart, W Nörtershäuser, J Papuga, and S Schmidt. Spins, Electromagnetic Moments, and Isomers $^{107-129}\text{Cd}$. *Phys. Rev. Lett.*, 110(19):192501, may 2013.
141. R F Garcia Ruiz, A R Vernon, C L Binnersley, B K Sahoo, M Bissell, J Billowes, T E Cocolios, W Gins, R P de Groote, K T Flanagan, A Koszorus, K M Lynch, G Neyens, C M Ricketts, K D A Wendt, S G Wilkins, and X F Yang. High-Precision Multiphoton Ionization of Accelerated Laser-Ablated Species. *Phys. Rev. X*, 8(4):41005, oct 2018.
142. M. Lindroos, M. Booth, D. Doran, Y. Koh, I. Oliveira, J. Rikowska, P. Richards, N. J. Stone, M. Veskovc,

- D. Zákoucký, and B. Fogelberg. Magnetic dipole moment of 127Sb and 129Sb by nuclear magnetic resonance on oriented nuclei. *Physical Review C - Nuclear Physics*, 53(1):124–126, 1996.
143. K. Kreim, M.L. Bissell, J. Papuga, K. Blaum, M. De Rydt, R.F. Garcia Ruiz, S. Goriely, H. Heylen, M. Kowalska, R. Neugart, G. Neyens, W. Nörtershäuser, M.M. Rajabali, R. Sánchez Alarcón, H.H. Stroke, and D.T. Yordanov. Nuclear charge radii of potassium isotopes beyond $N=28$. *Physics Letters B*, 731:97–102, apr 2014.
 144. M L Bissell, J Papuga, H Naidja, K Kreim, K Blaum, M De Rydt, R F Garcia Ruiz, H Heylen, M Kowalska, R Neugart, G Neyens, W Nörtershäuser, F Nowacki, M M Rajabali, R Sanchez, K Sieja, and D T Yordanov. Proton-Neutron Pairing Correlations in the Self-Conjugate Nucleus 38K Probed via a Direct Measurement of the Isomer Shift. *Phys. Rev. Lett.*, 113(5):52502, jul 2014.
 145. X F Yang, C Wraith, L Xie, C Babcock, J Billowes, M L Bissell, K Blaum, B Cheal, K T Flanagan, R F Garcia Ruiz, W Gins, C Gorges, L K Grob, H Heylen, S Kaufmann, M Kowalska, J Kraemer, S Malbrunot-Ettenauer, R Neugart, G Neyens, W Nörtershäuser, J Papuga, R Sánchez, and D T Yordanov. Isomer Shift and Magnetic Moment of the Long-Lived $1/2^+$ Isomer in ^{79}Zn : Signature of Shape Coexistence near ^{78}Ni . *Phys. Rev. Lett.*, 116(18):182502, may 2016.
 146. H. Heylen, C. Babcock, R. Beerwerth, J. Billowes, M. L. Bissell, K. Blaum, J. Bonnard, P. Campbell, B. Cheal, T. Day Goodacre, D. Fedorov, S. Fritzsche, R. F. Garcia Ruiz, W. Geithner, Ch. Geppert, W. Gins, L. K. Grob, M. Kowalska, K. Kreim, S. M. Lenzi, I. D. Moore, B. Maass, S. Malbrunot-Ettenauer, B. Marsh, R. Neugart, G. Neyens, W. Nörtershäuser, T. Otsuka, J. Papuga, R. Rossel, S. Rothe, R. Sánchez, Y. Tsunoda, C. Wraith, L. Xie, X. F. Yang, and D. T. Yordanov. Changes in nuclear structure along the Mn isotopic chain studied via charge radii. *Phys. Rev. C*, 94(5):54321, nov 2016.
 147. K Minamisono, D M Rossi, R Beerwerth, S Fritzsche, D Garand, A Klose, Y Liu, B Maaß, P F Mantica, A J Miller, P Müller, W Nazarewicz, W Nörtershäuser, E Olsen, M R Pearson, P.-G. Reinhard, E E Saperstein, C Sumithrarachchi, and S V Tolokonnikov. Charge Radii of Neutron Deficient $^{52,53}\text{Fe}$ Produced by Projectile Fragmentation. *Phys. Rev. Lett.*, 117(25):252501, dec 2016.
 148. G J Farooq-Smith, A R Vernon, J Billowes, C L Binnerley, M L Bissell, T E Cocolios, T Day Goodacre, R P de Groote, K T Flanagan, S Franchoo, R F Garcia Ruiz, W Gins, K M Lynch, B A Marsh, G Neyens, S Rothe, H H Stroke, S G Wilkins, and X F Yang. Probing the Ga ground-state properties in the region near $Z=28$ with high-resolution laser spectroscopy. *Phys. Rev. C*, 96(4):44324, oct 2017.
 149. M. Hammen, W. Nörtershäuser, D. L. Balabanski, M. L. Bissell, K. Blaum, I. Budinčević, B. Cheal, K. T. Flanagan, N. Frömmgen, G. Georgiev, Ch. Geppert, M. Kowalska, K. Kreim, A. Krieger, W. Nazarewicz, R. Neugart, G. Neyens, J. Papuga, P.-G. Reinhard, M. M. Rajabali, S. Schmidt, D. T. Yordanov, B. Cheal, K. T. Flanagan, N. Frömmgen, G. Georgiev, Ch. Geppert, M. Kowalska, K. Kreim, A. Krieger, W. Nazarewicz, R. Neugart, G. Neyens, J. Papuga, P.-G. Reinhard, M. M. Rajabali, S. Schmidt, and D. T. Yordanov. From Calcium to Cadmium: Testing the Pairing Functional through Charge Radii Measurements of $\text{Cd}^{100-130}$. *Physical Review Letters*, 121(10):102501, sep 2018.
 150. C. Gorges, L. V. V. Rodríguez, D. L. L. Balabanski, M. L. L. Bissell, K. Blaum, B. Cheal, R. F. F. Garcia Ruiz, G. Georgiev, W. Gins, H. Heylen, A. Kanellakopoulos, S. Kaufmann, M. Kowalska, V. Lagaki, S. Lechner, B. Maaß, S. Malbrunot-Ettenauer, W. Nazarewicz, R. Neugart, G. Neyens, W. Nörtershäuser, P.-G. Reinhard, S. Sailer, R. Sánchez, S. Schmidt, L. Wehner, C. Wraith, L. Xie, Z. Y. Y. Xu, X. F. F. Yang, and D. T. T. Yordanov. Laser Spectroscopy of Neutron-Rich Tin Isotopes: A Discontinuity in Charge Radii across the $N = 82$ Shell Closure. *Physical Review Letters*, 122(19):192502, may 2019.
 151. A. J. Miller, K. Minamisono, A. Klose, D. Garand, C. Kujawa, J. D. Lantis, Y. Liu, B. Maaß, P. F. Mantica, W. Nazarewicz, W. Nörtershäuser, S. V. Pineda, P. G. Reinhard, D. M. Rossi, F. Sommer, C. Sumithrarachchi, A. Teigelhöfer, and J. Watkins. Proton superfluidity and charge radii in proton-rich calcium isotopes. *Nature Physics*, 15(5):432–436, may 2019.
 152. L Xie, X F Yang, C Wraith, C Babcock, J Bieroń, J Billowes, M L Bissell, K Blaum, B Cheal, L Filippin, K T Flanagan, R F Garcia Ruiz, W Gins, G Gaigalas, M Godefroid, C Gorges, L K Grob, H Heylen, P Jönsson, S Kaufmann, M Kowalska, J Krämer, S Malbrunot-Ettenauer, R Neugart, G Neyens, W Nörtershäuser, T Otsuka, J Papuga, R Sánchez, Y Tsunoda, and D T Yordanov. Nuclear charge radii of $^{62-80}\text{Zn}$ and their dependence on cross-shell proton excitations. *Physics Letters B*, 797:134805, 2019.
 153. National Nuclear Data Center. *NNDC*. <https://www.nndc.bnl.gov/>, 2019.
 154. C. Babcock, H. Heylen, M. L. Bissell, K. Blaum, P. Campbell, B. Cheal, D. Fedorov, R. F. Garcia Ruiz, W. Geithner, W. Gins, T. Day Goodacre, L. K. Grob, M. Kowalska, S. M. Lenzi, B. Maass, S. Malbrunot-Ettenauer, B. Marsh, R. Neugart, G. Neyens, W. Nörtershäuser, T. Otsuka, R. Rossel, S. Rothe, R. Sánchez, Y. Tsunoda, C. Wraith, L. Xie, and X. F. Yang. Quadrupole moments of odd-A $^{53-63}\text{Mn}$: Onset of collectivity towards $N=40$. *Physics Letters, Section B: Nuclear, Elementary Particle and High-Energy Physics*, 760:387–392, 2016.
 155. X F Yang, Y Tsunoda, C Babcock, J Billowes, M L Bissell, K Blaum, B Cheal, K T Flanagan, R F Garcia Ruiz, W Gins, C Gorges, L K Grob, H Heylen, S Kaufmann, M Kowalska, J Krämer, S Malbrunot-Ettenauer, R Neugart, G Neyens, W Nörtershäuser, T Otsuka, J Papuga, R Sánchez, C Wraith, L Xie, and D T Yordanov. Investigating the large deformation of the $5/2^+$ isomeric state in ^{73}Zn : An indicator for triaxiality. *Phys. Rev. C*, 97(4):44324, apr 2018.
 156. M. Mougeot, D. Atanasov, K. Blaum, K. Chrysalidis, T. Day Goodacre, D. Fedorov, V. Fedosseev, S. George, F. Herfurth, J. D. Holt, D. Lunney, V. Manea, B. Marsh, D. Neidherr, M. Rosenbusch, S. Rothe, L. Schweikhard, A. Schwenk, C. Seiffert, J. Simonis, S. R. Stroberg, A. Welker, F. Wienholtz, R. N. Wolf, and K. Zuber. Precision Mass Measurements of Cr^{58-63} : Nuclear Collectivity Towards the $N=40$ Island of Inversion. *Physical Review Letters*, 120(23), jun 2018.

157. S. Michimasa, M. Kobayashi, Y. Kiyokawa, S. Ota, D. S. Ahn, H. Baba, G. P.A. Berg, M. Dozono, N. Fukuda, T. Furuno, E. Ideguchi, N. Inabe, T. Kawabata, S. Kawase, K. Kisamori, K. Kobayashi, T. Kubo, Y. Kubota, C. S. Lee, M. Matsushita, H. Miya, A. Mizukami, H. Nagakura, D. Nishimura, H. Oikawa, H. Sakai, Y. Shimizu, A. Stolz, H. Suzuki, M. Takaki, H. Takeda, S. Takeuchi, H. Tokieda, T. Uesaka, K. Yako, Y. Yamaguchi, Y. Yanagisawa, R. Yokoyama, K. Yoshida, and S. Shimoura. Magic Nature of Neutrons in Ca 54: First Mass Measurements of Ca 55-57. *Physical Review Letters*, 121(2), jul 2018.
158. M. P. Reiter, S. Ayet San Andrés, E. Dunling, B. Kootte, E. Leistenschneider, C. Andreoiu, C. Babcock, B. R. Barquest, J. Bollig, T. Brunner, I. Dillmann, A. Finlay, G. Gwinner, L. Graham, J. D. Holt, C. Hornung, C. Jesch, R. Klawitter, Y. Lan, D. Lascar, J. E. McKay, S. F. Paul, R. Steinbrügge, R. Thompson, J. L. Tracy, M. E. Wieser, C. Will, T. Dickel, W. R. Plaß, C. Scheidenberger, A. A. Kwiatkowski, and J. Dilling. Quenching of the N=32 neutron shell closure studied via precision mass measurements of neutron-rich vanadium isotopes. *Physical Review C*, 98(2), aug 2018.
159. A. Klose, K. Minamisono, A. J. Miller, B. A. Brown, D. Garand, J. D. Holt, J. D. Lantis, Y. Liu, B. Maaß, W. Nörtershäuser, S. V. Pineda, D. M. Rossi, A. Schwenk, F. Sommer, C. Sumithrarachchi, A. Teigelhöfer, and J. Watkins. Ground-state electromagnetic moments of Ca 37. *Physical Review C*, 99(6), jun 2019.
160. H. N. Liu, A. Obertelli, P. Doornenbal, C. A. Bertulani, G. Hagen, J. D. Holt, G. R. Jansen, T. D. Morris, A. Schwenk, R. Stroberg, N. Achouri, H. Baba, F. Browne, D. Calvet, F. Château, S. Chen, N. Chiga, A. Corsi, M. L. Cortés, A. Delbart, J. M. Gheller, A. Giganon, A. Gillibert, C. Hilaire, T. Isobe, T. Kobayashi, Y. Kubota, V. Lapoux, T. Motobayashi, I. Murray, H. Otsu, V. Panin, N. Paul, W. Rodriguez, H. Sakurai, M. Sasano, D. Steppenbeck, L. Stuhl, Y. L. Sun, Y. Togano, T. Uesaka, K. Wimmer, K. Yoneda, O. Aktas, T. Aumann, L. X. Chung, F. Flavigny, S. Franchoo, I. Gašparić, R. B. Gerst, J. Gibelin, K. I. Hahn, D. Kim, T. Koiwai, Y. Kondo, P. Koseoglou, J. Lee, C. Lehr, B. D. Linh, T. Lokotko, M. Mac-cormick, K. Moschner, T. Nakamura, S. Y. Park, D. Rossi, E. Sahin, D. Sohler, P. A. Söderström, S. Takeuchi, H. Törnqvist, V. Vaquero, V. Wagner, S. Wang, V. Werner, X. Xu, H. Yamada, D. Yan, Z. Yang, M. Yasuda, and L. Zanetti. How Robust is the N=34 Subshell Closure? First Spectroscopy of Ar 52. *Physical Review Letters*, 122(7), feb 2019.
161. X. Xu, M. Wang, K. Blaum, J. D. Holt, Yu A. Litvinov, A. Schwenk, J. Simonis, S. R. Stroberg, Y. H. Zhang, H. S. Xu, P. Shuai, X. L. Tu, X. H. Zhou, F. R. Xu, G. Audi, R. J. Chen, X. C. Chen, C. Y. Fu, Z. Ge, W. J. Huang, S. Litvinov, D. W. Liu, Y. H. Lam, X. W. Ma, R. S. Mao, A. Ozawa, B. H. Sun, Y. Sun, T. Uesaka, G. Q. Xiao, Y. M. Xing, T. Yamaguchi, Y. Yamaguchi, X. L. Yan, Q. Zeng, H. W. Zhao, T. C. Zhao, W. Zhang, and W. L. Zhan. Masses of neutron-rich Sc 52-54 and Ti 54,56 nuclides: The N=32 subshell closure in scandium. *Physical Review C*, 99(6), jun 2019.
162. E. Leistenschneider, M. P. Reiter, S. Ayet San Andrés, B. Kootte, J. D. Holt, P. Navrátil, C. Babcock, C. Barbi-
eri, B. R. Barquest, J. Bergmann, J. Bollig, T. Brunner, E. Dunling, A. Finlay, H. Geissel, L. Graham, F. Greiner, H. Hergert, C. Hornung, C. Jesch, R. Klawitter, Y. Lan, D. Lascar, K. G. Leach, W. Lippert, J. E. McKay, S. F. Paul, A. Schwenk, D. Short, J. Simonis, V. Somà, R. Steinbrügge, S. R. Stroberg, R. Thompson, M. E. Wieser, C. Will, M. Yavor, C. Andreoiu, T. Dickel, I. Dillmann, G. Gwinner, W. R. Plaß, C. Scheidenberger, A. A. Kwiatkowski, and J. Dilling. Dawning of the N=32 Shell Closure Seen through Precision Mass Measurements of Neutron-Rich Titanium Isotopes. *Physical Review Letters*, 120(6), feb 2018.
163. T. Motobayashi, Y. Ikeda, K. Ieki, M. Inoue, N. Iwasa, T. Kikuchi, M. Kurokawa, S. Moriya, S. Ogawa, H. Murakami, S. Shimoura, Y. Yanagisawa, T. Nakamura, Y. Watanabe, M. Ishihara, T. Teranishi, H. Okuno, and R F Casten. Large deformation of the very neutron-rich nucleus 32Mg from intermediate-energy Coulomb excitation. *Physics Letters B*, 346(1):9–14, 1995.
164. Tomoaki Togashi, Yusuke Tsunoda, Takaharu Otsuka, and Noritaka Shimizu. Quantum Phase Transition in the Shape of Zr isotopes. *Phys. Rev. Lett.*, 117(17):172502, oct 2016.
165. Mihai Horoi and Koblar A. Jackson. Signature of shape transition and shape coexistence in mesoscopic systems. *Chemical Physics Letters*, 427(1):147–152, aug 2006.
166. Gerda Neyens. Nuclear magnetic and quadrupole moments for nuclear structure research on exotic nuclei. *Reports on Progress in Physics*, 66(4):633–689, apr 2003.
167. J Wood. Simple Structure in Complex Nuclei. *Physics*, 6:52, 2013.
168. Ben Mottelson. Elementary modes of excitation in the nucleus. *Rev. Mod. Phys.*, 48(3):375–383, jul 1976.
169. Aage Bohr. Rotational motion in nuclei. *Reviews of Modern Physics*, 48(3):365–374, 1976.
170. James Rainwater. Background for the spheroidal nuclear model proposal. *Rev. Mod. Phys.*, 48(3):385–391, jul 1976.
171. J Papuga, M L Bissell, K Kreim, K Blaum, B A Brown, M De Rydt, R F Garcia Ruiz, H Heylen, M Kowalska, R Neugart, G Neyens, W Nörtershäuser, T Otsuka, M M Rajabali, R Sánchez, Y Utsuno, and D T Yordanov. Spins and Magnetic Moments of 49K and 51K Establishing the 1/2+ and 3/2+ Level Ordering Beyond N=28. *Phys. Rev. Lett.*, 110(17):172503, apr 2013.
172. J Papuga, M L Bissell, K Kreim, C Barbieri, K Blaum, M De Rydt, T Duguet, R F Garcia Ruiz, H Heylen, M Kowalska, R Neugart, G Neyens, W Nörtershäuser, M M Rajabali, R Sánchez, N Smirnova, V Somà, and D T Yordanov. Shell structure of potassium isotopes deduced from their magnetic moments. *Phys. Rev. C*, 90(3):34321, sep 2014.
173. R P de Groote, J Billowes, C L Binnarsley, M L Bissell, T E Cocolios, T Day Goodacre, G J Farooq-Smith, D V Fedorov, K T Flanagan, S Franchoo, R F Garcia Ruiz, Á Koszorús, K M Lynch, G Neyens, F Nowacki, T Otsuka, S Rothe, H H Stroke, Y Tsunoda, A R Vernon, K D A Wendt, S G Wilkins, Z Y Xu, and X F Yang. Dipole and quadrupole moments of 73-78Cu as a test of the robustness of the Z=28 shell closure near 78Ni. *Phys. Rev. C*, 96(4):41302, oct 2017.

174. Akito Arima and Hisashi Horie. Configuration Mixing and Magnetic Moments of Odd Nuclei. *Progress of Theoretical Physics*, 12(5):623–641, nov 1954.
175. Hisashi Horie and Akito Arima. Configuration Mixing and Quadrupole Moments of Odd Nuclei. *Physical Review*, 99(3):778–785, aug 1955.
176. A De-Shalit and I Talmi. *Nuclear Shell Theory*. Academic Press, New York, 1963.
177. C. Wraith, X.F. Yang, L. Xie, C. Babcock, J. Bieroń, J. Billowes, M.L. Bissell, K. Blaum, B. Cheal, L. Filippin, R.F. Garcia Ruiz, W. Gins, L.K. Grob, G. Gaigalas, M. Godefroid, C. Gorges, H. Heylen, M. Honma, P. Jönsson, S. Kaufmann, M. Kowalska, J. Krämer, S. Malbrunot-Ettenauer, R. Neugart, G. Neyens, W. Nörtershäuser, F. Nowacki, T. Otsuka, J. Papuga, R. Sánchez, Y. Tsunoda, and D.T. Yordanov. Evolution of nuclear structure in neutron-rich odd-Zn isotopes and isomers. *Physics Letters B*, 771:385–391, aug 2017.
178. M L Bissell, T Carette, K T Flanagan, P Vingerhoets, J Billowes, K Blaum, B Cheal, S Fritzsche, M Godefroid, M Kowalska, J Krämer, R Neugart, G Neyens, W Nörtershäuser, and D T Yordanov. Cu charge radii reveal a weak sub-shell effect at $N=40$. *Phys. Rev. C*, 93(6):64318, jun 2016.
179. R. Taniuchi, C. Santamaria, P. Doornenbal, A. Obertelli, K. Yoneda, G. Authalet, H. Baba, D. Calvet, F. Châteaueu, A. Corsi, A. Delbart, J.-M. Gheller, A. Gillibert, J. D. Holt, T. Isobe, V. Lapoux, M. Matsushita, J. Menéndez, S. Momiyama, T. Motobayashi, M. Niikura, F. Nowacki, K. Ogata, H. Otsu, T. Otsuka, C. Péron, S. Péru, A. Peyaud, E. C. Pollacco, A. Poves, J.-Y. Roussé, H. Sakurai, A. Schwenk, Y. Shiga, J. Simonis, S. R. Stroberg, S. Takeuchi, Y. Tsunoda, T. Uesaka, H. Wang, F. Browne, L. X. Chung, Z. Dombradi, S. Franchoo, F. Giacoppo, A. Gottardo, K. Hadyńska-Kłęk, Z. Korkulu, S. Koyama, Y. Kubota, J. Lee, M. Lettmann, C. Louchart, R. Olzeva, K. Matsui, T. Miyazaki, S. Nishimura, L. Olivier, S. Ota, Z. Patel, E. ahin, C. Shand, P.-A. Söderström, I. Stefan, D. Steppenbeck, T. Sumikama, D. Suzuki, Z. Vajta, V. Werner, J. Wu, Z. Y. Xu, and R Taniuchi Et al. ^{78}Ni revealed as a doubly magic stronghold against nuclear deformation. *Nature*, 569(7754):53, may 2019.
180. Tomoaki Togashi, Yusuke Tsunoda, Takaharu Otsuka, Noritaka Shimizu, and Michio Honma. Novel Shape Evolution in Sn Isotopes from Magic Numbers 50 to 82. *Physical Review Letters*, 121(6):062501, aug 2018.
181. A. Ekström, G. R. Jansen, K. A. Wendt, G. Hagen, T. Papenbrock, B. D. Carlsson, C. Forssén, M. Hjorth-Jensen, P. Navrátil, and W. Nazarewicz. Accurate nuclear radii and binding energies from a chiral interaction. *Physical Review C*, 91(5):051301, may 2015.
182. V Lapoux, V Somà, C Barbieri, H Hergert, J D Holt, and S R Stroberg. Radii and Binding Energies in Oxygen Isotopes: A Challenge for Nuclear Forces. *Phys. Rev. Lett.*, 117(5):52501, jul 2016.
183. S Ettenauer. Laser spectroscopy of neutron-rich antimony isotopes. *In preparation*, 2020.
184. Á Koszorús, X F Yang, J Billowes, C L Binnersley, M L Bissell, T E Cocolios, G J Farooq-Smith, R P de Groote, K T Flanagan, S Franchoo, R F Garcia Ruiz, S Geldhof, W Gins, A Kanellakopoulos, K M Lynch, G Neyens, H H Stroke, A R Vernon, K D A Wendt, and S G Wilkins. Precision measurements of the charge radii of potassium isotopes. *Phys. Rev. C*, 100(3):34304, sep 2019.
185. Á Koszorús and Others. Charge radii of potassium isotopes, nuclear forces, and the magic character of neutron number $N = 32$. *In preparation*, 2020.
186. R. P. de Groote, J. Billowes, C. L. Binnersley, M. L. Bissell, T. E. Cocolios, T. Day Goodacre, G. J. Farooq-Smith, D. V. Fedorov, K. T. Flanagan, S. Franchoo, R. F. Garcia Ruiz, W. Gins, J. D. Holt, Á. Koszorús, K. M. Lynch, T. Miyagi, W. Nazarewicz, G. Neyens, P.-G. Reinhard, S. Rothe, H. H. Stroke, A. R. Vernon, K. D. A. Wendt, S. G. Wilkins, Z. Y. Xu, and X. F. Yang. Measurement and microscopic description of odd-even staggering of charge radii of exotic copper isotopes. *Nature Physics*, pages 1–5, apr 2020.
187. A Vernon and Others. No Title. *In preparation*, 2019.
188. R. F. Garcia Ruiz, A. R. Vernon, C. L. Binnersley, B. K. Sahoo, M. Bissell, J. Billowes, T. E. Cocolios, W. Gins, R. P. de Groote, K. T. Flanagan, A. Koszorus, K. M. Lynch, G. Neyens, C. M. Ricketts, K. D. A. Wendt, S. G. Wilkins, and X. F. Yang. Laser Spectroscopy of exotic indium ($Z = 49$) isotopes: Approaching the $N = 50$ and $N = 82$ neutron numbers. Technical report, CERN, the European Organization for Nuclear Research, Geneva, 2017.
189. R F Garcia Ruiz, C Gorges, M Bissell, K Blaum, W Gins, H Heylen, K Koenig, S Kaufmann, M Kowalska, J Krämer, P Lievens, S Malbrunot-Ettenauer, R Neugart, G Neyens, W Nörtershäuser, D T Yordanov, and X F Yang. Development of a sensitive setup for laser spectroscopy studies of very exotic calcium isotopes. *Journal of Physics G: Nuclear and Particle Physics*, 44(4):044003, apr 2017.
190. M. Thoennessen. Exploring new neutron-rich nuclei with the facility for rare isotope beams. *Nuclear Data Sheets*, 118(1):85–90, 2014.
191. Hans Werner Hammer, Andreas Nogga, and Achim Schwenk. Colloquium: Three-body forces: From cold atoms to nuclei. *Reviews of Modern Physics*, 85(1):197–217, jan 2013.
192. Kristina D Launey, Tomas Dytrych, and Jerry P Draayer. Symmetry-guided large-scale shell-model theory. *Progress in Particle and Nuclear Physics*, 89:101–136, 2016.
193. G Hagen, M Hjorth-Jensen, G R Jansen, and T Papenbrock. Emergent properties of nuclei from ab initio coupled-cluster calculations. *Physica Scripta*, 91(6):63006, may 2016.
194. E. Caurier, G. Martínez-Pinedo, F. Nowacki, A. Poves, and A. P. Zuker. The shell model as a unified view of nuclear structure. *Reviews of Modern Physics*, 77(2):427–488, jun 2005.
195. S Leoni, B Fornal, S Ujenuic, and C A Ur. Multifaceted Quadruplet of Low-Lying Spin-Zero States in ^{66}Ni : Emergence of Shape Isomerism in Light Nuclei. *Phys. Rev. Lett.*, 118(16):162502, apr 2017.